Carbon 223 (2024) 118970

Contents lists available at ScienceDirect

Carbon

journal homepage: www.elsevier.com/locate/carbon

Hydrogel-integrated graphene superstructures for tissue engineering: From periodontal to neural regeneration

Iman Zare [a], Mojdeh Mirshafiei [b], Bahareh Kheilnezhad [c], Bahareh Farasati Far [d], Mahnaz Hassanpour [e], Esmail Pishbin [f,g], Shahrzad Sadat Eftekhar Vaghefi [h,i], Fatemeh Yazdian [j], Hamid Rashedi [b], Anwarul Hasan [k,l,**], Xiangdong Wang [m], Mohsen Adeli [n,*], Pooyan Makvandi [o,p,q,***]

[a] Research and Development Department, Sina Medical Biochemistry Technologies Co., Ltd., Shiraz, 7178795844, Iran
[b] Department of Biotechnology, School of Chemical Engineering, College of Engineering, University of Tehran, Tehran, Iran
[c] Department of Chemical Engineering, The Pennsylvania State University, University Park, PA, 16802, United States
[d] Department of Chemistry, Iran University of Science and Technology, Tehran, Iran
[e] Department of Chemistry, Institute for Advanced Studies in Basic Sciences (IASBS), Zanjan, 45137-66731, Iran
[f] Nano-Bioengineering Lab, Department of Mechanical Engineering, Sharif University of Technology, Azadi Ave., Tehran, 11365-11155, Iran
[g] Bio-microfluidics Lab, Department of Electrical Engineering and Information Technology, Iranian Research Organization for Science and Technology, Tehran, Iran
[h] Pathology and Stem Cell Research Center, Kerman University of Medical Sciences, Kerman, Iran
[i] Department of Physiology, Kerman Medical Science Branch, Islamic Azad University, Kerman, Iran
[j] Department of Life Science Engineering, Faculty of New Science and Technologies, University of Tehran, Tehran, Iran
[k] Department of Mechanical and Industrial Engineering, Qatar University, Doha, 2713, Qatar
[l] Biomedical Research Center, Qatar University, Doha, 2713, Qatar
[m] Department of Pulmonary and Critical Care Medicine, Zhongshan Hospital, Fudan University Shanghai Medical College, Shanghai, 200032, China
[n] Department of Chemistry and Biochemistry, Freie Universitat Berlin, Takustrasse 3, Berlin, 14195, Germany
[o] The Quzhou Affiliated Hospital of Wenzhou Medical University, Quzhou People's Hospital, 324000, Quzhou, Zhejiang, China
[p] Centre of Research Impact and Outreach, Chitkara University, Rajpura, 140417, Punjab, India
[q] Department of Biomaterials, Saveetha Dental College and Hospitals, SIMATS, Saveetha University, Chennai, 600077, India

ARTICLE INFO

Keywords:
Hydrogel
Graphene
Tissue engineering
Regenerative medicine
Two-dimensional materials

ABSTRACT

Hydrogel-integrated graphene superstructures (GSSs) represent a promising platform for applications in tissue engineering and regenerative medicine. Graphene, a two-dimensional carbon-based material, possesses remarkable mechanical, thermal, and electrical characteristics, making it a strong candidate for application in biomedicine. Researchers have pursued the integration of graphene with hydrogels, known for their biocompatibility and ability to provide a conducive environment for cellular growth, to craft sophisticated scaffolds tailored to tissue engineering needs. The integration of hydrogels and graphene enables the construction of 3D frameworks that closely mimic the natural extracellular matrix (ECM) found in biological tissues. Hydrogels furnish a biocompatible, well-hydrated environment, while the graphene component bolsters the scaffold's mechanical integrity and electrical conductivity. This amalgamation enhances cellular adhesion, differentiation, and proliferation, thereby facilitating tissue regeneration. A notable advantage of hydrogel-integrated GSSs lies in their capacity to support the growth and differentiation of a variety of cell types such as PC12, MG-63, U-87, and MC3T3-E1 cell lines. Overall, hydrogel-integrated GSSs exhibit great potential for advancing biomimetic tissue engineering and regenerative medicine. The combination of the unique properties of graphene with the biocompatibility of hydrogels enables the development of advanced scaffold systems for tissue regeneration. Further research and development in this domain will play a crucial role in advancing regenerative medicine and the treatment of various diseases and injuries.

* Corresponding author.
** Corresponding author. Department of Mechanical and Industrial Engineering, Qatar University, Doha, 2713, Qatar.
*** Corresponding author. The Quzhou Affiliated Hospital of Wenzhou Medical University, Quzhou People's Hospital, 324000, Quzhou, Zhejiang, China.
E-mail addresses: hasan.anwarul.mit@gmail.com (A. Hasan), adeli.m@lu.ac.ir (M. Adeli), pooyanmakvandi@gmail.com (P. Makvandi).

https://doi.org/10.1016/j.carbon.2024.118970
Received 13 November 2023; Received in revised form 23 February 2024; Accepted 24 February 2024
Available online 26 February 2024

1. Introduction

The lives of millions of patients suffering from incurable diseases have been saved through organ transplantation since the 1950s [1], and the demand for this procedure has outstripped the supply of donors. To meet the demands of transplantable organs for the growing numbers of patients awaiting transplantation, an alternative is urgently needed. It is important to note that the immune system can sometimes reject the transplanted organs. Tissue engineering represents an interdisciplinary and promising field in biomedical engineering, offering new solutions for the reconstruction of tissues and organs affected by disease or injury [2,3]. In this context, scientists have utilized natural and synthetic polymer-based biomaterials in tissue engineering with suitable structures to replicate the native ECM [4], thus facilitating the restoration of tissue structures and functions [5,6]. Hydrogels are one of the most prevalent types of biomaterials offering 3D micro and macro environments [2,7,8] with several unique characteristics, including hydrophilicity, rapid swelling, high swelling percentages (>90% water molecules from aqueous solutions without dissolving in the solution), and tunable pores [9], connectivity of pores, and softness. A hydrogel may also consist of micropores or nanopores that enable ions or small/macro biomolecules to diffuse into and out of the gel's surroundings [8,10,11].

Despite the numerous attributes of hydrogels, such as their favorable chemical properties (*e.g.*, degradation), physical characteristics (*e.g.*, biomechanical properties, porosity, diffusion), and biological features (affecting cell behavior and growth factor release), achieving the stimulation of tissue and organ regeneration depends on the degree of crosslinking and the choice of polymers used [12]. The process of crosslinking contributes to the formation of gel network pores and influences its mechanical attributes [9]. Consequently, it becomes a complex endeavor to facilitate cell proliferation and migration when the pore size of conventional hydrogels (nm scale) does not align with the dimensions of cells. Because most hydrogels have a low intrinsic modulus, stabilizing macroporous or microporous structures modeled after extracellular matrix morphology is challenging [9]. Conversely, researchers discovered that some of the crosslinkers used in the manufacturing of crosslinked hydrogels are toxic [2,13–15], expensive [2,14,15], and inaccessible [15]. As additional components are integrated to serve as crosslinkers, antibacterial agents, bioactive signals, and intelligent agents, the process of manufacturing hydrogels becomes progressively more demanding.

Recently, the effects of carbon-based nanocomposites on tissue engineering scaffolds have been considered [16–18]. Likewise, graphene and its related materials have become valuable components in the realm of hydrogel-based graphene, finding applications in diverse biomedical disciplines. These applications include drug delivery [19], biosensors [20], photothermal therapy (PTT) for treating tumors [11], bioimaging [21], and scaffolds for tissue engineering [22]. It is possible to integrate graphene into polymeric hydrogels. Graphene can give hydrogels some unique properties that common hydrogels do not possess [23]. Graphene serves two purposes in hydrogels: (1) it acts as a gelator for self-assembly and (2) it serves as a filler or crosslinker used to combine small molecules with macromolecules to prepare multipurpose hydrogels. These multifunctional features include pH [24] and photo-thermal response [11], self-healing, antibacterial [24] with excellent mechanical [25], and high electrical properties [25], which are referred to as graphene-integrated hydrogel [26]. Furthermore, graphene-based hydrogels are easy to modify and functionalize, allowing them to be used in biocompatible applications. In this overview, we will explore the use of graphene and its modified counterparts as biomaterials, with a particular focus on their manufacturing processes, composition, and the primary attributes commonly applied in the field of biomedicine.

2. Basic principles

An increasing interest has been shown in developing 3D tissue engineering scaffolds based on carbon-based nanomaterials, which are known for their excellent physiochemical properties [27,28]. Carbon-based nanomaterials include graphene as their fundamental structure, serving as a critical element that encompasses a variety of modifications with diverse configurations and characteristics. These adaptations encompass graphene oxide (GO), reduced graphene oxide (rGO), graphene quantum dots (GQDs), and ultra-thin layers of graphene, either singular or in limited numbers [28,29]. The integration of graphene and its variations into hydrogels has been pursued to enhance the characteristics of traditional hydrogels, such as mechanical strength and chemical, physical, and biological attributes, to enable new and exceptional functionalities. These outstanding functions contain high electrical conductivity [30], being smart hydrogel [31], high capacity of drug loading [32,33], mitigation of inflammatory response, and the tendency to the absorption, binding, and delivery of biomolecule [32,34,35]. A variety of allotropes of carbon-based materials can be found in the following list [11,36] (Fig. 1): zero-dimensional (fullerene), rolled one-dimensional (carbon nanotube), two-dimensional (graphene and its derivatives GO and rGO), and stacked three-dimensional (diamond and graphite) [37,38].

2.1. Structures and integration process of graphene derivatives with hydrogels

Derived from graphene, GO possesses a profusion of oxygen-functional groups. The –OH groups and epoxides are predominantly located within the basal plane, while carbonyl and carboxyl groups (*e.g.*, –COOH, and -*O*-) are primarily distributed along the periphery of the GO structure [35,39–41]. Covalent bonds are established through interactions among these functional groups, while non-covalent interactions manifest as a result of hydrogen bonding and electrostatic attractions occurring between GO and chemically active agents [42,43]. The carboxyl functional groups of graphene contribute to maintaining colloidal stability and generate a surface charge that is responsive to pH variations [33,44].

Notably, GO composition hydrogels form under certain conditions and it would be best to modify/functionalize GO before GO gels are formed, because under an acidified solution most carboxyl groups are protonated and neutralized. Furthermore, the presence of the repulsive force between GO sheets at physiological pH makes GO composition gel unstable [45]. Therefore, precise consideration should be given to the preparation of the hydrogel formulation method containing GO regarding GO and other used biomolecules and biomaterials. Additional chemical groups, specifically hydroxyl and epoxide groups found on the graphene surface, remain uncharged but possess polarity, resulting in the formation of feeble interactions, hydrogen bonding, and additional chemical reactions [44]. GO contains an abundance of oxygen-based groups, facilitating its dispersion in both water and various organic solvents, while also enhancing material compatibility and reactivity [46,47]. In addition, GO's higher reactivity may lead to significant biotransformations that alter its physicochemical properties, which potentially interfere with biomedical applications [48,49].

On the other hand, a chemical or thermal treatment of GO results in rGO. Since rGO contains few oxygen and hydrophilic functional groups, it is insoluble in water and difficult to bind hydrophilic polymers to it [50]. The dispersibility of rGO relies on the extent of reduction, signifying that r-GO with progressive reduction and varying oxygen levels exhibits poor dispersibility. In contrast, GO demonstrates superior water dispersibility and stability in polar solutions compared to rGO. A direct approach to crafting hydrogels based on rGO involves the hydrothermal and chemical reduction of GO sheets *in situ*, either in aqueous or organic solvents [51,52]. Throughout the reduction process, the oxygen-containing functional groups are significantly diminished, fostering potent hydrophobic interactions among the sheets of rGO. These interactions, in turn, lead to the segregation of rGO sheets from the solution, culminating in gel formation [51,53]. As a result of rGO,

the primary modes of adsorption and physical forces involve non-covalent interactions, specifically π–π interactions, hydrophobic interactions, van der Waals forces, and electrostatic interactions. These interactions have the potential to facilitate the binding between polymeric hydrogels and small biomolecules [35,50]. When compared to GO, rGO exhibits a reduced number of hydrogen bonds and electrostatic interactions, resulting in decreased protein adsorption and altered cellular responses [40]. In addition, rGO features a lower surface charge density, resulting in a diminished thrombogenic effect [54]. Intriguingly, rGO has the capability to elevate the levels of reactive oxygen species within biological systems, a phenomenon that may play a pivotal role in angiogenesis [55], given that ROS can function as significant biological signaling molecules [56].

2.2. Non-covalent bonds effect on the structure

Surface modification via non-covalent bonds primarily involves interactions such as π–π bonding, hydrogen bonding, ionic interactions, and electrostatic attraction modification. The process of functionalizing through non-covalent bonds is straightforward and occurs under mild conditions [42]. Non-covalent interactions, like hydrogen bonding and hydrophobic interactions, have been harnessed due to their versatility as key drivers for hydrogel formation [57]. For instance, when GO and PVA aqueous solutions are mixed, vigorously shaken for 10 s, and sonicated for 20 min, it results in the formation of a hybrid GO/PVA hydrogel. The crosslinking phenomenon is initiated by hydrogen bonding between the hydroxyl-rich PVA chains and the oxygen-containing groups on the GO sheets. Moreover, GO exhibits a negative surface charge within the physiological pH range (approximately ~7.35–7.45), which enhances not only hydrogen bonding but also electrostatic forces, hydrophobic interactions, and π–π stacking interactions. These non-covalent forces create a strong affinity for GO to accommodate biomolecules like proteins, enzymes, antibodies, and DNA fragments commonly present in serum-based culture media, thereby influencing subsequent cellular responses [35,40].

Various crosslinking agents are employed for GO gelation, including DNA, proteins, synthetic polymers with positive charges, hydrogen bonding properties, and metal ions (*e.g.*, Ca^{2+}, Mg^{2+}, Fe^{2+}, Sr^{2+}). The crosslinkers are strategically employed to balance electrostatic repulsion, hydrophobic forces, and hydrogen interactions within GO-based colloid suspensions. The responsiveness of non-covalent bonds to external stimuli (*e.g.*, temperature and pH variations), the degree of oxidation, and GO's negative charge may have either positive or negative effects on secondary protein structures. This can result in structural alterations and diminished protein activity [58] or influence the binding and delivery of biomolecules/proteins. The selection of specific GO features can be tailored to mitigate strong interactions with proteins and preserve protein conformation.

2.3. Covalent bond's effect on the structure

Covalent bonds enhance the processability of an object and enable it to perform new functions. Covalently functionalizing GO can be accomplished in several ways, including hydroxyl functionalization and carboxyl functionalization [42]. Protein covalently attaches to GO on the surface of hydrogels that exhibit resistance to heat, pH fluctuations, storage conditions, and organic solvents. This covalent bonding significantly augments the durability of the protein-GO conjugate [59,60]. The remarkable stability of injectable GO hydrogels results in their prolonged retention in various organs, including the lungs, spleen, liver, and bone marrow, leading to challenges in clearance and diminished biocompatibility within the body [61].

2.4. Mechanical properties

A high water content can lead to reduced mechanical strength in hydrogels [62]. Hydrogels can benefit from the presence of oxygen-containing functional groups and the extensive specific surface area of GO, which can enhance their mechanical properties. Hydrophilic groups present in polymer chains have the potential to improve the mechanical characteristics of GO sheets by forming hydrogen bonds with oxygen-related groups [63]. As hydrogels deform, their bonds can be continuously broken and reformed to accommodate the new deformation state. In a particular study, methacrylate was functionalized using GO (referred to as MeGO) to enable covalent bonding between GO and methacrylate gelatin (GelMA) hydrogel [64]. Mechanical testing demonstrated a substantial increase in the hydrogel's elastic modulus, indicating enhanced toughness, as the concentration of MeGO rose from 0 to 3.0 mg/mL. In addition, when MeGO is integrated into the polymeric network, the material can expand under external forces and dissipate energy without weakening the structure and increasing fracture resistance [64]. MeGO does not affect hydrogel stiffness, which is a key determinant of cell behavior in GelMA. In GelMA, the only use of GO causes distortions of the polymeric matrix, resulting in fractures and limited mechanical properties due to the wrinkled structure [65].

Due to the low energy of hydrogen bonds, they are easily recovered following a disconnection. As the hydrogels are deformed, the GO layer exhibits sufficient flexibility, regardless of whether it is a single layer or a few layers. Hydrogels can adapt well to deformation and form new hydrogen bonds with the matrix polymer, which increases their tensile strength [63]. In addition to hydrogen bonds, hydrogels' mechanical characteristics benefit from the substantial surface area of GO,

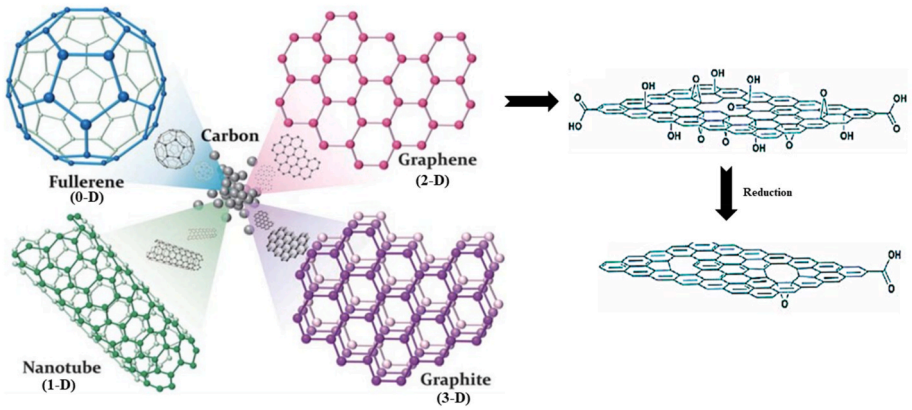

Fig. 1. Schematic illustrating the atomic arrangement of various carbon allotropes including graphene (GR), graphene oxide (GO), and reduced graphene oxide (rGO). Reproduced with permission from Ref. [37]. Copyright (2018), Elsevier. Ref. [38]. Copyright (2010), John Wiley & Sons. (A colour version of this figure can be viewed online.)

facilitating its interaction with hydrophilic polymers and further enhancing their mechanical properties [63]. Due to the low energy of hydrogen bonds, they can rapidly reform after being disrupted. Consequently, GO improves the mechanical features of composite hydrogels while preserving their tensile strength. Furthermore, single-layer and few-layer GO demonstrate remarkable flexibility [63].

2.5. Biodegradability

Until now, the degradation potential of GO has not been thoroughly examined, despite its significance in determining the destiny of foreign substances within living systems, particularly in hydrogels, a critical phase in the clearance process of GO from the body. GO undergoes degradation not only through oxidative processes involving hydrogen peroxide and eosinophil peroxidase during the inflammatory response in affected regions [45,66] but can also be enzymatically degraded by myeloperoxidase within 24 h [66]. Degradation is dependent on the colloidal stability of the suspension, indicating that GO's hydrophilic nature plays an important role in enzyme degradation [66,67].

2.6. Electrical conductivity

The property of rGO is that it is a very hard material, which is able to conduct electricity well, as opposed to GO-rich which contains oxygen as an electrical isolator. The reduction of GO results in the partial restoration of the SP^2 structure, leading to a significant increase in rGO's conductivity [68–70]. RGO has a remarkable electrical conductivity of approximately 6600 S cm^{-1} and a remarkable mobility of 320 $cm^2/(V{\cdot}s)$, making it highly versatile and applicable in a number of electronic applications [68–70]. These fields include electronics devices (*e.g.*, batteries), biosensors, and tissue regeneration applications. While the oxygen content in GO structure leads to increased density defects, which can diminish electroconductivity, this has significant implications in various domains, notably in the realm of tissue regeneration [39,45].

Although other conductive biomaterials like polyaniline (PANI) [3] and polypyrrole (PPy) have been explored, rGO has emerged as the most prominent candidate for rendering hydrogels conductive. In the medical field, conductive hydrogels, characterized by their high water content, have been designed to emulate the electrophysiological milieu of biological tissues for tissue repair, including applications in neural [71], skeletal muscle [72], cardiovascular [73], and skin [3,74]. For instance, in a study focusing on nerve tissue regeneration, silk fibroin blended with GO (SF/GO) was electrospun, followed by *in situ* chemical post-reduction to produce SF/rGO composites [75]. The presence of rGO significantly enhanced the overall conductivity, reaching approximately $\sim 4 \times 10^{-5}$ S cm^{-1} in the dry state and peaking at $\sim 3 \times 10^{-4}$ S cm^{-1} in the hydrated state when compared to GO [75]. Electrospinning scaffolds were assessed in a dry/hydrated state to determine their conductivity during fabrication and implantation. The conductivity of natural tissue can be adjusted via graphene derivatives; particularly rGO whose properties include providing a range of human tissue conductivity between 1×10^{-6} and 8×10^{-5} S cm^{-1} [76,77].

3. graphene derivatives incorporated innovative biomaterials for hard tissue regeneration

Recent research has highlighted a growing interest in the utilization of hydrogel-integrated GSSs for utilization in tissue engineering and regenerative medicine (Fig. 2). These structures combine the exceptional mechanical properties of graphene with the biocompatibility and water-retention capabilities of hydrogels, making them well-suited for promoting tissue regeneration [78]. Hydrogel-integrated GSSs offer several advantages over conventional tissue engineering approaches [79]. For example, compared to other materials commonly used in tissue engineering, such as collagen (Col) or elastin, graphene has better mechanical properties. This makes graphene-based scaffolds more durable and able to support cell and tissue growth. Conversely, hydrogels possess an exceptional water-retaining capacity and demonstrate biocompatibility, thus creating a soft and hydrated milieu conducive to cell growth, akin to the natural ECM found in living tissues. By combining GSSs with hydrogels, it becomes possible to customize surface properties and geometries, allowing for precise manipulation of cellular behavior and tissue development. This advancement greatly enhances the potential for successful tissue integration and regeneration, enabling the engineering of complex tissues and organs that closely resemble their natural counterparts [80,81].

On the other hand, graphene composites offer an excellent option for developing various composite inks with a wide range of functions. Graphene-based inks can be customized to possess specific properties such as biocompatibility, photo responsiveness, electrical conductivity, or hydrophilicity [82]. During the printing process, it is important to have a low coefficient of friction, which can be achieved by using graphene fillers. This ensures smooth and accurate deposition with minimal defects [83]. Graphene or graphene-reinforced composite inks have the potential to be highly effective in the 3D manufacturing industry, provided that proper parameterization and reciprocal relationships are established between the printable material and the printing technique [84,85]. Graphene or composite inks reinforced with graphene have the potential to be valuable assets in the 3D manufacturing industries. However, it is crucial to establish parameters and define relationships between the printable material's properties and the printing technique used. Despite this, the development of cell-laden bioinks enhanced with graphene is still in its early stages [85]. Due to the remarkable electrical properties of graphene, many ongoing studies focus on creating

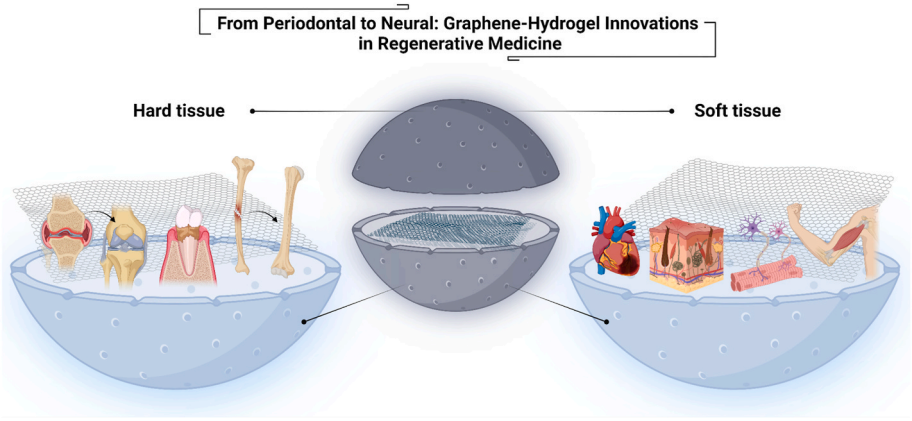

Fig. 2. Schematic depiction of hydrogel-integrated graphene: a revolution in tissue engineering from periodontal to neural regeneration. (A colour version of this figure can be viewed online.)

conductive bioinks for nerve [86,87], muscle regeneration [88], and cardiovascular tissue [89].

Complex tissue structures with precise control can now be created using three-dimensional bioprinting technologies in an automated manner. However, the currently fabricated structures are unable to accurately replicate the dynamic nature of tissues. Tissue regeneration and repair in nature often involve changes in the conformation of the tissue structure [90]. Therefore, it is necessary to incorporate time-dependence into 3D-printed tissue constructs to mimic the structural changes that occur in tissues. To achieve this, four-dimensional (4D) bioprinting has been developed. This technique utilizes stimuli-responsive biomaterials and cell traction forces to create structurally dynamic tissue constructs. The ability to create such dynamic structures would allow the creation of tissue structures that are capable of undergoing morphological changes [91]. One material that has been used in the ink for 3D printing is graphene. Graphene provides printed constructs with electroconductive properties. Therefore, graphene-based nanomaterials have the potential to be used in bioinks for 4D bioprinting. In addition, other carbon-based nanobiomaterials, such as carbon nanotubes (CNTs), can also be used to create bioinks that respond to electrical stimuli for 4D bioprinting [92]. The range of potential applications for graphene-based hydrogel superstructures is extensive. They offer promising prospects for advancing the regeneration of diverse tissues, including but not limited to bone, cartilage, skin, and nerve tissues. This section aims to shed light on the well-documented research and utilization of hydrogel-integrated GSSs in the realm of both hard and soft tissue regeneration.

3.1. Hard tissue

3.1.1. Bone reconstruction

Bone is a complex bioceramic composite connective tissue that produces blood cells, stores minerals, as well as forms the skeleton that supports and protects the tissues and organs. The hierarchical architecture of bone tissue contributes to its mechanical properties, enables mass exchange, and maintains cell activity [93,94]. The organic integrity of the bone structure provides an inherent self-healing ability, however, self-healing is typically limited in complex clinical conditions where excessive amounts of bone are required or the regenerative process is impaired [95–97]. Even though allografts and autografts remain the primary solution for regenerating bone defects, using autografts is invasive, expensive, and can result in hematomas and infections that frequently affect both the donor and surgical sites [98]. Allografts also pose problems such as potential immune rejection, infectious pathogenesis, and reduced osteoinductivity [99]. Accordingly, it becomes essential to devise innovative methods to surpass current restrictions and create materials for bone replacement that can comprehensively restore bone functionality [97].

It is ideal for a bone graft to be biocompatible and to contain no toxic effects on the host tissue either locally or systemically and provide appropriate porosity for cell and tissue ingrowth. Furthermore, it exhibited mechanical compatibility with the host bone's characteristics and featured biodegradability at a regulated rate that aligns with the promotion of fresh bone formation [100]. Hydrogels are widely employed as three-dimensional (3D) scaffolds due to their high extensibility, flexibility, and excellent biocompatibility [101]. For bone tissue engineering, hydrogels need to meet some primary requirements including compatibility with tissue and cells, osteoconductive activity, and osteoinductive activity [102]. On the contrary, substances employed in bone tissue engineering must typically possess a combination of robust mechanical resilience and the ability to promote bone growth. Hydrogels, commonly employed as bone tissue substitutes, often exhibit limited mechanical strength, necessitating enhancement [103]. Supramolecular integrated hydrogels can mimic key properties of ECM and offer strong attachment to the bone in therapeutically relevant conditions such as bleeding, bodily fluid, and uneven surfaces. Since they have exceptional cohesive mechanical properties in terms of strength, stiffness, and toughness, bone-integrated functional hydrogels could guarantee proper hard tissue fixation [104].

Graphene-based materials find extensive application, either independently or in conjunction with bone implants and scaffolds, to enhance bone regeneration. They achieve this by promoting cell adhesion, proliferation, and osteoblastic differentiation while reinforcing mechanical properties [105]. The introduction of graphene into hydrogels has exhibited remarkable performance, not only simplifying three-dimensional handling but also substantially expediting cell differentiation, all without the need for extra bone growth agents. Furthermore, strategies aimed at mitigating the robust pi-pi interactions between graphene sheets enhance the dispersion of these sheets within polymers. Consequently, it is anticipated that the incorporation of graphene and its derivatives into materials for bone regeneration has the potential to stimulate both biomineralization and the differentiation of cells toward an osteogenic lineage, thus enhancing osteoconductivity [106–108].

Considering the impressive positive effects on bone regeneration resulting from the combination of GO and sericin, Jiang et al. devised an injectable hydrogel composed of alginate-tyramine, sericin, and GO (Alg/Ser/GO). This hydrogel was cross-linked enzymatically using HRP/H_2O_2. Intriguingly, an increase in the GO content led to a reduction in the storage modulus of the hydrogel. Beyond a critical strain of 20%, the hydrogel underwent structural collapse. Analysis of the compressive stress-strain curves for Alg/Ser/20GO revealed a compression modulus of 16.5 kPa and a compressive strength of 68 kPa at 36% strain. Furthermore, the results from scratch assays demonstrated that both Alg/Ser and Alg/Ser/20GO hydrogels significantly increased the covered areas, suggesting that sericin could induce macrophage migration. This, in turn, enhanced the infiltration and polarization of M2 macrophages, ultimately promoting the osteoblastic differentiation of BMSCs. It is worth noting, however, that GO may have the potential to induce inflammation and toxicity, particularly at concentrations exceeding 20 μg/mL. Both *in vitro* and *in vivo* experiments utilizing Alg/Ser/GO hydrogels resulted in macrophage infiltration into neighboring tissues, effectively mitigating inflammation and preventing the thickening of fibrous capsules. Moreover, GO significantly contributed to expediting the expansion, promoting osteogenic specialization, and enhancing mineral deposition in rat BMSCs [109].

To enhance the physicochemical attributes and encourage attachment, proliferation, and osteogenic differentiation of rat bone marrow-derived mesenchymal stem cells (rBMSCs), Wang et al. introduced GO into zwitterionic hydrogels (which is synthesized using maleic anhydride as the crosslinking agent and grafted the zwitterionic material on maleilated chitosan (CS) via click chemistry). The incorporation of GO into these zwitterionic hydrogels, known for their robust mechanical properties and slow degradation rate, resulted in a reduced release rate of GO and lower cytotoxicity. Remarkably, in both *in vitro* and *in vivo* settings, the combination of GO and zwitterions demonstrated a synergistic effect, promoting rBMSC proliferation and osteogenic differentiation [108].

In another investigation, Jiao et al. engineered a biomimetic composite by amalgamating gelatin with rGO. This composite exhibited double-phase properties, including exceptional biocompatibility for controlling progenitor cell differentiation, serving as a carrier for delivering bioactive signals, and functioning as a nanofiller for photo-crosslinked hydrogels (Fig. 3A and B). Composites incorporating an optimal quantity of rGO harnessed the advantages of both gelatin and rGO, leading to an enhanced structural morphology of the biomimetic callus. These composite materials exhibited the capability to promote bi-differentiation of bone marrow-derived mesenchymal stem cells (BMSCs), expediting the process of bone regeneration. This transformation of composite structure from porous to blocky was visually evident in scanning electron microscopy (SEM) images (Fig. 3C). The precise ratio of rGO in these composite materials effectively controlled

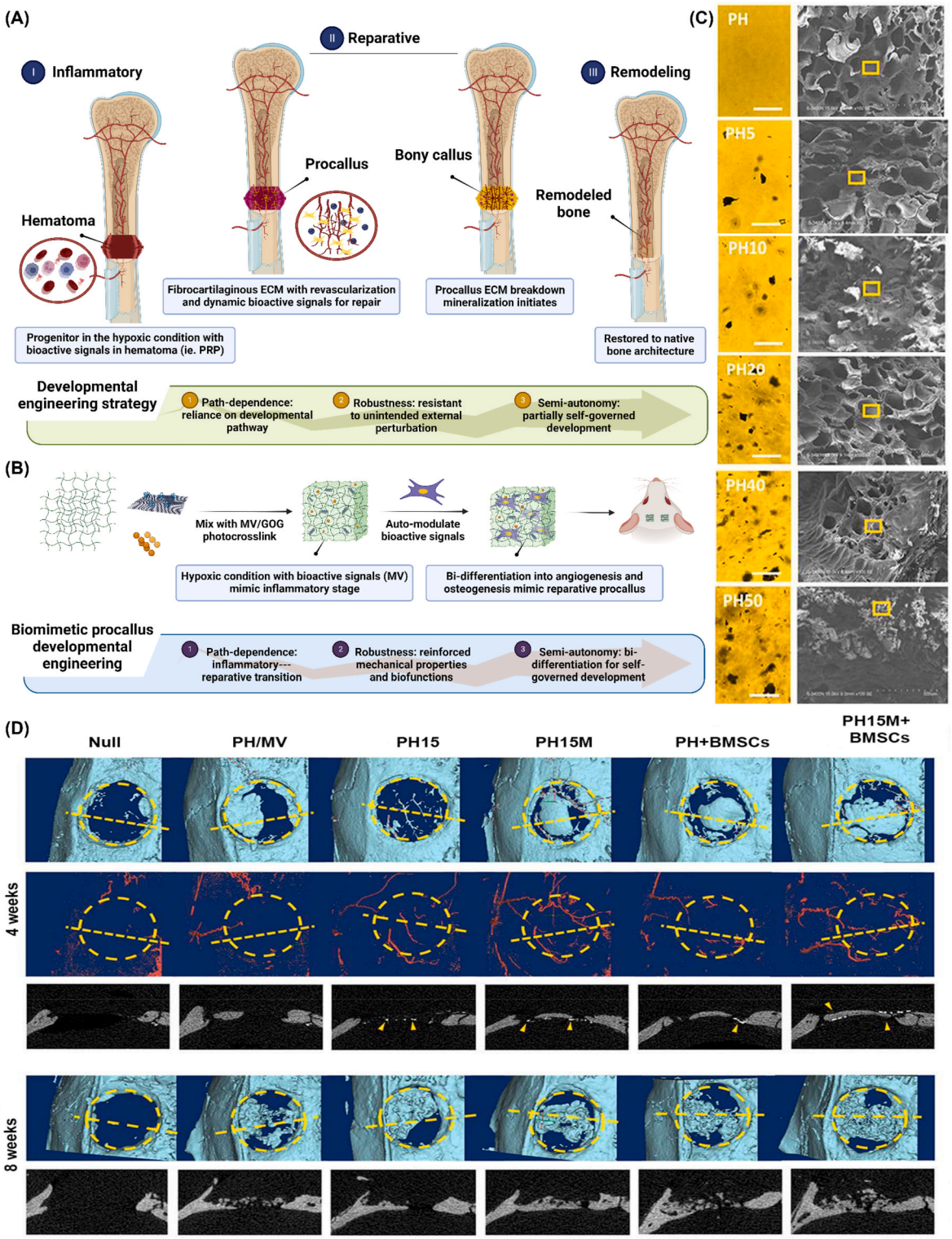

Fig. 3. (A) Schematic representation of the bone healing process and the developmentally engineered strategy's path-dependent, robust, and semi-autonomous nature for biomimetic procallus. (B) Schematic diagram depicting the biomimetic procallus within the realm of developmental engineering. The biomimetic microstructure of the composites is modulated by GOG. (C) SEM image of a cross-sectional view of the composite, alongside a light view of the hydrogel. Scale bar: 100 μm. (D) Evaluation of rat calvarial defect repair by the biomimetic procallus using μCT analysis at 4 weeks and 8 weeks. The yellow dotted lines indicate the location of the section view below the reconstructed 3D views, while the yellow arrowheads point to newly formed blood vessels perfused with contrast media, displaying higher radiodensity compared to the bone. Reproduced with permission from Ref. [110]. Copyright (2021), Elsevier. (A colour version of this figure can be viewed online.)

their mechanical properties, maintaining them within a suitable range for facilitating adhesion and proliferation of BMSCs. In addition, an assessment of gene expressions related to endothelial markers, which included Ang1, VEGF, vWF, and CD31, was conducted to illustrate the angiogenic differentiation of BMSCs when cultured on these diverse composites. Interestingly, the PH30 M composite exhibited an inhibitory effect on the formation of tubules by BMSCs. Intriguingly, cells forming capillary-like structures expressed the endothelial cell marker CD31, confirming the composite's capability to induce angiogenic differentiation in BMSCs. As callus progenitors differentiated, early hypoxia-induced angiogenesis gradually alleviated hypoxic stress and promoted subsequent bone formation (Fig. 3D) [110]. Table 1 shows further examples of hydrogel-integrated graphene in bone tissue engineering.

3.1.2. Cartilage regeneration

Cartilage, a specialized type of connective tissue, possesses a unique combination of smoothness and elasticity. Its composition primarily includes Col fibers, glycosaminoglycans, proteoglycans, and a substantial proportion of water, thereby providing vital structural support within the body. During embryonic development, cartilage plays a pivotal role as a template for the formation of bone and retains its presence as an integral component of the adult skeletal system [111]. This tissue manifests in three primary forms within the human body: hyaline or articular cartilage, fibrocartilage, and elastic cartilage. These variations are distinguished by their differing concentrations of Col II and proteoglycans, each contributing to distinct physiological functions. It is a relatively simple tissue, devoid of nerves, lymphatics, and blood vessels, with a sparse cell density, primarily chondrocytes, that provide nutrients by diffusion [112]. The inherent limitation of chondrocytes' ability to proliferate and the absence of a natural supply of healthy chondrocytes to repair defects restricts the spontaneous regeneration or self-healing process [113]. Cartilage damage not only poses a significant financial and psychological burden to the patient, but in severe cases, it can also lead to deformity, joint degeneration, and disability. In such situations, it becomes necessary to intervene therapeutically to address articular cartilage defects. Current therapeutic techniques for repairing and/or regenerating cartilage tissue include microfracture therapy, autologous chondrocyte implantation, osteochondral autografts and allografts, and cartilage transplantation [114].

Hydrogels hold promise as biomaterials for cartilage tissue engineering due to their ability to replicate key features of the native extracellular environment. Achieving adequate mechanical strength is a crucial consideration in designing hydrogels for cartilage regeneration. Conventional hydrogel networks, however, often rely on a single polymer, resulting in diminished mechanical properties that do not match those of natural cartilage [115]. Graphene incorporation into hydrogels for the development of tissue engineering scaffolds is rooted in a range of beneficial properties, encompassing its large surface area, ease of functional group modifications, remarkable tensile strength, and exceptional electrical conductivity. Likewise, it creates a cell-friendly microenvironment and effectively induces the differentiation of mesenchymal stem cells (MSCs) into chondrocyte lineages like hyaline cartilage [114,116]. On the other hand, GO exhibits unique attributes of anti-wear and self-lubrication, owing to its low effective threshold and high surface-to-volume ratio. To achieve both the mechanical robustness and ideal lubrication properties resembling those of native articular cartilage, Trucco et al. initiated a study focused on incorporating GO into a bilayered hydrogel matrix comprising gellan gum and polyethylene glycol diacrylate (PEGDA). This bilayered construct comprised two distinctive hydrogel layers, each with precise thicknesses, mirroring the mechanical traits of healthy articular cartilage. The outcomes of this investigation unveiled the affirmative impact of introducing GO into the upper layer, as validated by tribological assessments. Notably, this nanocomposite bolstered mechanical attributes, particularly enhancing toughness. Furthermore, a comprehensive evaluation over six days revealed no cytotoxic repercussions on human chondrocytes, underscoring the biocompatibility and safety of this bilayered hydrogel system [79].

In an alternative investigation, Hou et al. successfully crafted a biomimetic hydrogel integrating GO nanosheets, modified anionic polyurethane (nGO-APU), and polyvinyl alcohol (PVA) using a novel approach involving freeze-thaw and annealing processes. The hydrogel's primary scaffold consisted of annealed PVA (a-PVA), which provided essential mechanical support, while interwoven nGO-APU chains contributed to water retention and lubrication properties. This synergistic combination not only resisted compressive loads, ensuring long-lasting energy absorption, but also closely replicated the performance of the natural temporomandibular joint (TMJ) disc. Following implantation into a rabbit's TMJ for a duration of up to 24 weeks, the nGO-APU/a-PVA hydrogel retained its structural integrity, effectively shielded against cartilage wear, and mitigated the progression of osteoarthritis. Finite element analysis (FEA) additionally highlighted the hydrogel's effectiveness in dispersing stress and managing energy dissipation during real-world loading scenarios [117].

In another important study, Fu et al. introduced an innovative approach to create a hydroxyapatite (HA) composite coating with unique self-lubricating and antibacterial features. Their method involved combining GO hybrid pseudopolyrotaxane (PPR) supramolecular hydrogels through vacuum infiltration, followed by a self-assembly process induced by a host-guest interaction. These hybrid hydrogels, which contained vancomycin, were embedded within a textured HA coating, resulting in sustained drug release. They also displayed a remarkable gel-sol transition triggered by the application of shear force and the generation of frictional heat. This particular phenomenon emulates the extrusion of synovial fluid that occurs during the movement of articular cartilage. As a result, it led to outstanding anti-wear and self-lubricating performance, along with promising antibacterial properties effective against *Staphylococcus aureus*. Significantly, the friction coefficient and wear rate of these composite coatings exceeded those of textured HA coatings by almost fivefold and were notably higher by three orders of magnitude, respectively. This substantial enhancement in performance can be attributed to the synergistic lubrication facilitated by cyclodextrin-based supramolecular PPR hydrogels and GO lubricants [118].

Graphene-based hydrogels have shown the potential to enhance the development of type II Col, facilitating the proliferation of chondrocytes and the remodeling of the cartilage matrix. To investigate the impact of graphene-based hydrogels on cartilage regeneration and the role of scaffold porosity in chondrocyte mobility and matrix remodeling during matrix-induced chondrogenesis, Lyu et al. engineered a graphene elastic hydrogel (GEH) framework using freeze-casting methods with partially rGO suspensions (Fig. 4A). In contrast to numerous alternative biomaterials, GEH maintains its structural integrity after formation and exhibits resistance to a broad spectrum of biological enzymes. Moreover, it swiftly restores its initial shape even after undergoing repetitive compression in a physiological saline environment (Fig. 4B). When chondrocytes were cultured on these hydrogel scaffolds, a noticeable increase in both metalloproteinase production and their inhibitors was observed, implying that the GEH scaffold creates an environment conducive to cartilage matrix remodeling. Histological staining also demonstrated a marked difference in the distribution of regenerated cartilage tissue between GEH scaffolds and their dehydrated counterparts, underscoring the significance of a porous structure on the scaffold's outer surface in promoting cartilage regeneration (Fig. 4C) [119]. Table 1 provides a summary of key findings related to the application of hydrogel-integrated graphene in cartilage tissue engineering.

3.1.3. Periodontal regeneration

The complex periodontal tissue, which encompasses both soft and hard components, surrounds and supports teeth. It consists of a sophisticated hierarchical structure, including the alveolar bone,

Table 1
Hydrogel-integrated graphene applications in hard tissue engineering and regenerative medicine.

Application	Type of graphene	Cell line (*in vitro*) or animal models (*in vivo*)	Composition	Preparation	Characterization	Outcomes	Refs.
Bone	GO	rBMSCs	HA/GO/CS	Self-assembly & simultaneous reduction & crosslinking	XPS, TGA, H NMR, FTIR, WAXD, FESEM, TEM, dynamic rheological tests, porosity study, fluorescence image, cell viability, DNA contents	•Exceptional mechanical resilience, strong adhesion properties of HA, excellent porosity, and favorable biocompatibility.	[172]
	GO	BMSCs	Silk fibroin/GO	Crosslinking	XRD, FT-IR, XPS, SEM, porosity analysis, compressive strength, LSCM images, phalloidin-DAPI staining, proliferation assay, ALP activity, alizarin red staining	•Promoting orderly arrangement of SF & mechanical properties by addition of GO • Efficient utilization of GO promotes the differentiation of stem cells into the osteogenic lineage	[173]
	GO	BMSCs/Rats	miR-29b/GO-PEG-PEI−CS	Encapsulation	FTIR, elemental analysis, zeta potentials, average sizes, TEM, TGA, CCK-8 assay, gel retardation assay, LSCM, fluorescent image, ALP activity, CT, histological analysis	• Enhance osteogenic differentiation of BMSCs and facilitate bone regeneration while minimizing inflammatory responses	[174]
	GO	rBMSCs & C3H10T1/2 & MG-63	CS/GP/GO	Lyophilization	TEM, XRD, FTIR, SEM, Raman spectroscopy, porosity & swelling study, protein adsorption & biodegradation study, DAPI stained, MTT assay, FDA stained, alizarin red stained, real-time RT-PCR	• Retaining its thermosensitivity & injectability even after the addition of GO • Significant improvement in protein adsorption & swelling abilities after the addition of GO • Controlling the degradation behavior of hydrogel • Facilitating osteogenic differentiation of mMSCs	[175]
	Graphene	rBMSCs/Rats	Bulk graphene material with a self-supporting graphene hydrogel (SGH) structure	Filtration	SEM, XRD, DMTA, DAPI, MTT assay, live/dead double staining, ROS level study, HE staining, ALP assay, immunofluorescence staining, alizarin red S staining	• Improve cell adhesion, spreading, and proliferation • Formation of new blood vessel • High biocompatibility & bone regeneration without any external inducer	[176]
	GO	MG63 & NIH-3T3/male Albino-Wistar rats	GO−IONPs−nHAP, -fibrin	Sol-gel/ lyophilization	SEM, EDAX, FTIR, swelling & biodegradation study, protein adsorption study, porosity analysis, *in vitro* biomineralization assay, MTT assay, H & E staining, Masson's trichrome stain, alizarin red staining, ALP assay	• Integrating GO into the hydrogel enhanced the scaffold's porous structure, mimicking the natural ECM of bone tissue • This improvement contributed to the scaffold's structural stability, regulated degradation, and heightened its osteoinductive capabilities	[177]
	rGO	OVX-BMSCs/ rats	CS/rGO	Electrodeposition	SEM, FTIR, Raman, cell proliferation assay, ALP staining assay, RT-PC, western blot assay, pulsatile delivery, drug loading & photothermally drug release, micro-CT, sequential fluorescent labeling, H&E, Masson's trichrome staining, DAPI staining, TRAP staining & blood vessels immunofluorescence labeling	• A remarkable effect of CS/ rGO film on bone regeneration by biomimetic administration of teriparatide • Enhancing blood vessel density within the newly generated bone and the central defect region • Reducing unintended systemic adverse effects while facilitating osteoporotic bone regeneration	[178]
	rGO	MG-63 & rBMSCs/adult male Sprague Dawley rats	nHA−rGO	*In situ* self-assembly	TEM, AFM, SEM, FTIR, XPS, qRT-PCR, H&E staining, micro-CT, NIR thermal image, live/dead stain, proliferation study, ALP staining, VG staining, TRAP staining	• Excellent physicochemical properties, biocompatibility, photothermal conversion efficiency, & osteoinductive ability • The photothermal effect of nHA-rGO scaffolds can effectively kill MG-63 cells • The nHA-rGO scaffold potently inhibits tumor	[179]

(*continued on next page*)

Table 1 (*continued*)

Application	Type of graphene	Cell line (*in vitro*) or animal models (*in vivo*)	Composition	Preparation	Characterization	Outcomes	Refs.
						growth under NIR laser irradiation • The nHA-rGO scaffold can simultaneously promote rBMSC proliferation and differentiation	
Cartilage	GO	C28/12	Gelatin-genipin/CS−GO	Lyophilization	SEM, FTIR, porosity & swelling study, compressive strength, Young's modulus, toughness, MTT assay, *in vitro* degradation	• With increasing GO concentration, structural and mechanical properties improved • The pore size, distribution of pores, and tensile strength closely resemble those found in natural articular cartilage extracellular matrix	[180]
	Graphene	Chondrocyte	PCL-graphene (PG)−PVA-glycerol (Pg)	Freeze thawing/3D bioprinting	SEM, XRD, FTIR, DSC, TGA, XPS, porosity measurement, water content, swelling ratio, Finite element simulation, mechanical tests, drug loading & release, tribological tests	• The favorable mechanical characteristics are akin to those of native load-bearing cartilage • Offering drug release and on-demand photothermal conversion capabilities • Excellent biocompatibility and low cell adhesion	[181]
	GO	NIH-3T3 & hMSC	GO/alginate	Crosslinking	FTIR, TEM, mechanical analysis, live/dead assay, safranin O red/alcian blue staining, DMA	• Remarkable enhancement in the compressive stiffness of GO/Alg hydrogel, reaching levels similar to articular tissue • Biocompatibility of suspended GO flakes • Improving viability of enclosed within the hydrogels	[182]
	GO	hBMSCs	GO/PDLLA	Photocrosslinking	AFM, SEM, FTIR, Raman, swelling ratio, Young's modulus, live/dead Staining, real-time RT-PCR, DNA contents, histological analysis, total Col and sulfated GAG quantitative analysis, sulfated GAG alcian blue assay, type II Col, and insulin immunostaining	• Improving mechanical properties and chondrogenic differentiation • Increased expression of cartilage matrix genes, including aggrecan and type II Col • The pro-chondrogenic impact of GO became more pronounced as the GO concentration increased	[183]
	GO	hADMSCs	Alginate- gelatin-chondroitin sulfate/GO	3D printing	ATR-FTIR, H NMR, UV-VIS, TEM, FESEM, POM, FTIR, XRD, water content, swelling ratio, rheological measurements, Mechanical properties, Alamar blue assay, live/dead assay, fluorescence staining, immunofluorescence staining	• Improve printability, higher fidelity, and resolution by incorporating GO • Excellent cell growth, alignment, & distribution within the GO-contained scaffold • High cytocompatibility & bioactivity • Chondrogenic differentiation without exogenous pro-chondrogenic factors	[184]
	GO	N.A.	PVA/GO−PEG	Freezing/thawing	FTIR, Raman, XRD, TEM, Rheological measurements, mechanical properties, dynamic compressive behaviors, friction & wear topography	• Improving mechanical strength and toughness • Creation of a robust and densely reinforced double network structure with high load-bearing capacity • High mechanical properties and excellent lubricity simultaneously	[185]

cementum, and periodontal ligament (PDL). The primary objective of periodontal therapy is the efficient restoration of compromised periodontal tissue [120,121]. However, existing clinical methods for periodontal tissue regeneration, such as guided tissue regeneration and bone grafts, face limitations in their applicability, particularly in cases of intraosseous defects and class II fissure defects. Furthermore, their regenerative potential is restricted due to their intricate technical requirements [122]. Recent investigations have suggested that the properties and makeup of hydrogels play a pivotal role in influencing the restoration of periodontal tissue [120]. Hydrogels can also serve as a carrier for the transportation of human dental pulp stem cells (hDPSCs), facilitating the restoration of damaged dentin and pulp tissues [123]. To

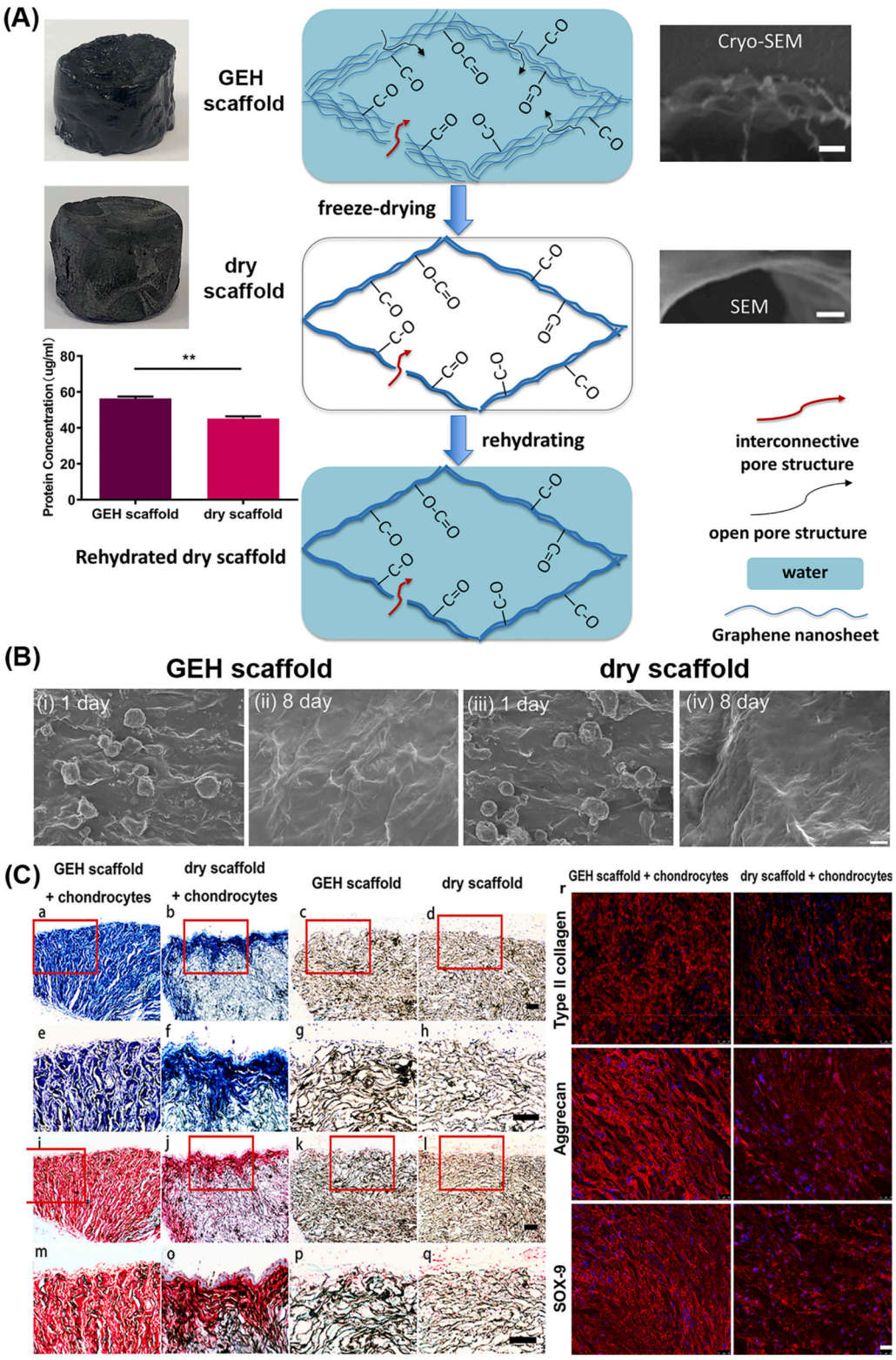

Fig. 4. (A) Illustration depicting the characteristics of the dry scaffolds and GEH (Graphene-Enhanced Hydrogel) scaffold. The GEH scaffold showcases an interconnected pore structure, open pore configuration, substantial surface area, and moderate oxygen content. (B) SEM images demonstrating scaffold surfaces at 1 and 8 days post-seeding. (C) Histological staining of chondrocyte-seeded GEH and dry scaffolds 8 weeks after implantation, using Toluidine blue and Safranin O/fast green, with cell-free scaffolds as controls. Higher magnification images (e–h) correspond to the boxed regions in (a–d), respectively. (i–q) Higher-magnification images correspond to the respective boxed areas in (i and l). (r) Immunofluorescence staining for type II Col, aggrecan, and SOX-9 in dry and chondrocyte-seeded GEH scaffolds at 8 weeks post-implantation. Reproduced with permission from Ref. [119]. Copyright (2022), American Chemical Society. (A colour version of this figure can be viewed online.)

design suitable scaffolds that support periodontal ligament stem cells' (PDLSCs') proliferation rate, allow for good cell engrafting, and preserve cell viability, Vera-Sánchez et al. successfully developed graphene and silk-fibroin constructs. Graphene provided differentiation capacity, while SF prevented inflammatory response and also offered GO better handling and 3D properties. The result demonstrated that in the absence of any growth factors, hPDLSCs differentiated more favorably into osteo/cementoblasts [124].

To expedite the process of periodontal bone regeneration and regulate the inflammatory periodontal environment in diabetic conditions, Li et al. introduced a conductive scaffold made of alginate and gelatin enriched with hydroxyapatite nanoparticles (PHA) and polydopamine (PDA)- mediated GO (PGO). As Fig. 5A and B demonstrated, PGO and PHA were obtained using a one-step PDA functionalization strategy. In order to create an immunomodulatory scaffold for periodontal bone regeneration in diabetics, PDA functionalization made it possible for the PHA and PGO to be evenly distributed in an alginate and gelatin network (Fig. 5C and D). The PGO in the scaffold served as a conductive pathway, giving the scaffold conductivity. This conductivity allowed the scaffold to transmit natural electrical signals to cells, which then activated Ca^{2+} channels (Fig. 5E). Moreover, the combination of cell adhesion and reactive oxygen species (ROS)-scavenging properties of PDA synergistically provided the scaffold with immunomodulatory activity (Fig. 5F). The conductivity and immunomodulatory activity synergistically promoted alveolar bone regeneration in the diabetic inflammatory periodontal microenvironment (Fig. 5G). The addition of PGO improved the conductivity of the scaffold (Fig. 5H) and also promoted cell spreading (Fig. 5I). This helped transmit natural electrical signals to the cells, leading to the activation of Ca^{2+} channels (Fig. 5J). Besides, reduction in the polarization of M1 macrophages, a decrease in the production of inflammatory cytokines, and the activation of M2 macrophages. Consequently, cytokines associated with osteogenesis were secreted. Micro-CT analysis revealed that at 28 days after surgery, the PGO-PHA-AG group's bone mineral density was higher than that of the other groups (Fig. 5K) [125].

In a separate effort to promote the proliferation and differentiation of hDPSCs into osteoblasts, Amiryaghoubi et al. developed an injectable thermosensitive hydrogel composed of a GO and a copolymer based on poly(N-isopropylacrylamide) (PNIPAAm), with varying proportions of CS. This synthesized hydrogel effectively induced the expression of osteogenic genetic responses like osteocalcin (OCN) and Runx2, while also enhancing alkaline phosphatase (ALP) activity and calcium deposition [126]. Table 1 furnishes a comprehensive summary of the multifaceted applications of hydrogel-integrated graphene in hard tissue engineering and regenerative medicine.

4. Graphene derivatives incorporated innovative biomaterials for soft tissue engineering applications

4.1. Dermal wound healing and skin regeneration

Human skin, being the body's largest organ, plays a pivotal role in

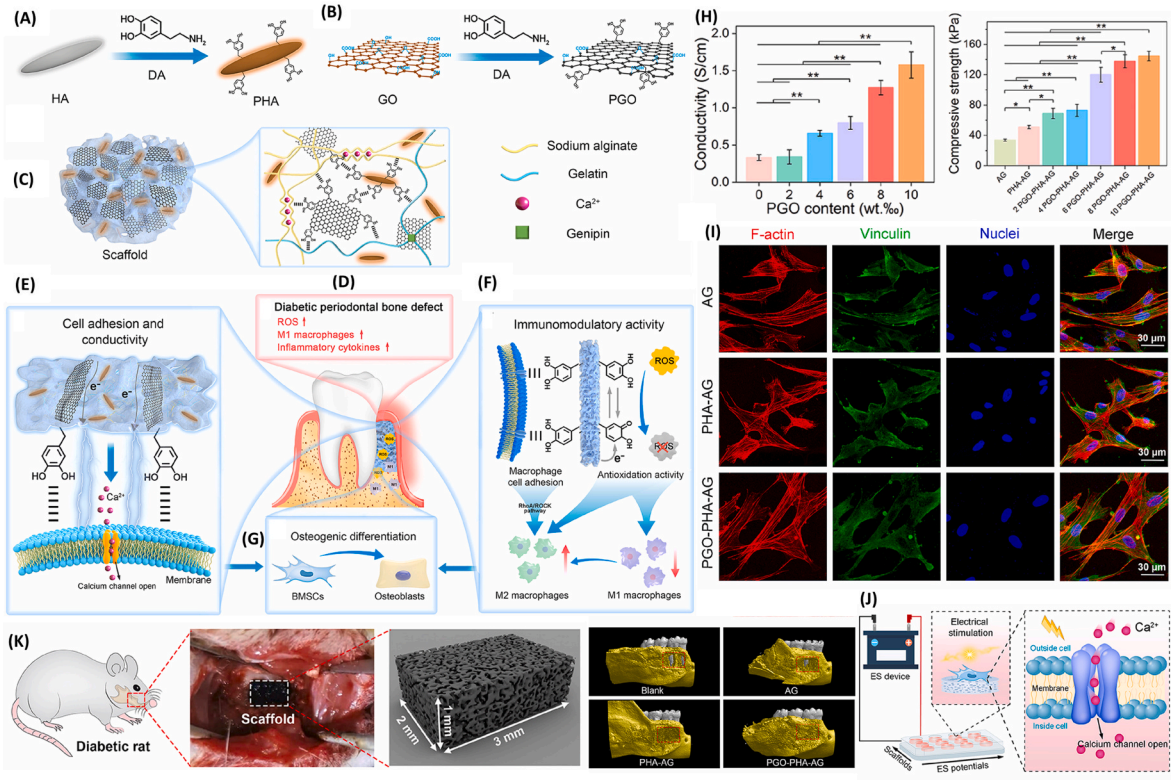

Fig. 5. Schematic represents the synthesis of the PGO-PHA-AG scaffold with multifunctional properties for potential application in periodontal bone regeneration in diabetes. (A) Schematic of PHA synthesis. (B) Schematic of PGO synthesis. (C) Scheme of interactions in the physicochemical double-bridged PGO-PHA-AG scaffold network. (D) ROS, M1 macrophages, and inflammatory cytokines are overexpressed in the local diabetic periodontal microenvironment. (E) The scaffold promoted cell adhesion and transmitted endogenous electrical signals to cells, thereby activating Ca^{2+} channels. (F) The cell-adhesive and ROS-scavenging properties of PDA endowed the scaffolds with the immunomodulatory activity that decreased M1 macrophage polarization and activated M2 macrophages secreting osteogenesis-related cytokines. (G) Conductivity and immunomodulatory activity synergistically promoted periodontal bone regeneration. (H) Scaffold conductivities with various PGO contents. Compressive strength of the AG, PHA-AG, and PGO-PHA-AG scaffolds. (I) Cell morphology of BMSCs on the surface of AG, PHA-AG, and PGO-PHA-AG scaffolds. (J) Schematic of high-throughput ES. Conductive scaffolds delivered electrical signals to BMSCs, causing Ca^{2+} influx. (K) Surgical procedure for implanting scaffolds in a diabetic rat periodontal defect model. Micro-CT image of the rat mandible at the implantation site. Reproduced with permission from Ref. [125]. Copyright (2022), Elsevier. (A colour version of this figure can be viewed online.)

multiple essential physiological functions, including immunity, metabolism, substance absorption and excretion, and sensory functions. However, being the body's first line of defense and having a soft and elastic nature, the skin is prone to various types of damage. However, as the body's first physical defense as well as its soft and elastic nature, skin is highly susceptible to a wide range of damage. While minor injuries can be naturally repaired by the body through Col and fibrin production, severe irreversible wounds necessitate the use of skin substitutes for treatment [127]. Hydrogels have recently gained popularity as ideal materials for wound dressings, as they facilitate traumatic autolytic debridement, regulate moisture levels, protect wounds against external infections, and prevent secondary damage due to soft tissue fragility and localized stress. In particular, adhesive supramolecular hydrogels play a vital role as quick-acting hemostatic agents or sealants, effectively halting the escape of fluids at the point of application. This attribute is of utmost importance in various emergencies [128,129].

Conductive polymers like graphene and its derivatives have shown potential in promoting the growth of fibroblasts and keratinocytes. They offer promising prospects in the field of skin tissue engineering and wound healing, owing to their extensive surface area, protein adsorption capabilities, and antibacterial characteristics [42,130]. For instance, Khan et al. devised a cost-effective and readily available composite hydrogel. They achieved this by crosslinking GO-functionalized arabinoxylan with PVA through tetraethyl orthosilicate (TEOS) via straightforward blending techniques. Numerous oxygen-based functional groups and the large surface area enhanced cell survival and proliferation as well as facilitated cell adhesion to hydrogels through hydrogen bonding. On the other hand, its sharp edges can rupture bacterial membranes, hindering their activity and replication. Therefore, this hydrogel exhibited improved antibacterial properties against various bacterial strains. Furthermore, it exhibited notable efficacy in anticancer evaluations and demonstrated biocompatibility with U-87 and MC3T3-E1 cell lines, a result of the combined synergistic effects [131].

By incorporating dispersed peptide-coated graphene (PCG) within the hydrogel framework, Xue et al. devised and crafted a single-layer hydrogel artificial skin. Peptide self-assembly fostered dynamic and resilient interactions within the hydrogel network, while the nearby graphene sheets acted as conductive layers for micro-capacitors. The material between these graphene layers acted as the dielectric, resulting in a hydrogel with remarkable stretchability, ultra-sensitive mechanical sensing capabilities, and rapid self-healing abilities. These hydrogels exhibited the ability to extend up to 77 times their original length and undergo self-recovery within minutes [132].

In a different investigation, Zhao et al. designed a flexible hydrogel dressing tailored for adaptable wound care, offering effective antibacterial properties through a gentle photothermal mechanism (Fig. 6A). They developed a hydrogel, by phenylboronic acid-functionalized graphene (rGB) sheets and carboxymethyl CS decorated with quaternary ammonium salts (QAS). This hydrogel exhibits a unique combination of covalent and noncovalent bonds, which imparts it with adaptable mechanical properties, robust tissue adhesion, and remarkable self-healing capabilities when applied to dynamic wounds. In addition, the hydrogel incorporating phenylboronic acid-functionalized rGB mimicked the glycocalyx and selectively captured multiple surface bacterial colonies. Subsequently, the quaternary CS (QCS) disrupted the bacterial membranes, achieving effective antibacterial action via a gentle photothermal effect at low temperatures (Fig. 6B). Consequently, the use of hydrogel as an *in vivo* wound dressing to inhibit methicillin-resistant *Staphylococcus aureus* (MRSA) infection and accelerate dynamic wound healing is anticipated (Fig. 6C) [133].

4.2. Neural simulation and regeneration

The human neural tissue, known for its complexity, comprises the peripheral nervous system (PNS) with neurons spread throughout the body and the central nervous system (CNS) consisting of the brain and spinal cord. Both of these function in tandem to regulate homeostasis and respond to external stimuli. While minor injuries to the PNS can heal and regenerate spontaneously, more severe injuries may necessitate surgical intervention. Conversely, the CNS is significantly more complex and rarely recovers naturally from damage. Thus, the ability of neural tissues to regenerate is comparatively limited [134,135].

The incorporation of chemical compounds or molecules (*e.g.*, TEMPO, photosensitive, *etc.*), within the hydrogels offers great potential as an alternative approach for neural tissue treatment. These hydrogels have the ability to successfully fill irregular neural tissue defects, providing a conducive environment for repair and regeneration. Moreover, hydrogels enable the transmission of mechanical signals to neural cells, which facilitate cell division, proliferation, and paracrine activity, all of which are crucial for neural tissue regeneration [136–138]. In a study conducted by Rezaei et al., GO was introduced into a Col hydrogel scaffold to enhance the biological characteristics of neural stem/precursor cells (NS/PC). Their findings showed that the incorporation of 1–1.5% GO led to improved NS/PC survival, migration, neurite outgrowth, cell spreading, and clustering, with a more pronounced effect observed in Col/GO hydrogels. GO played a role in enhancing interactions between neural stem cells and Col by providing micro/nanostructures and unique physicochemical cues, which improved the interfaces for cell-material interactions. In addition, GO influenced the elasticity of Col hydrogels in a manner conducive to neural stem cell growth [139]. Similarly, Liu et al. developed an electrically conductive hydrogel by covalently embedding carbon nanotube poly(ethylene glycol) acrylate (CNTpega) and GO acrylate (GOa) within oligo(polyethylene glycol fumarate) (OPF) hydrogels through chemical crosslinking. Subsequently, a reduction process was carried out within an L-ascorbic acid solution to reduce GOa. The resultant hydrogel displayed excellent biocompatibility and notably boosted PC12 cell proliferation, cell spreading, and the development of neurites [140].

In another study, Amagat et al. explored the effectiveness of neural differentiation guidance through the use of an anisotropic conductive hydrogel based on graphitic carbon nitride (g-C_3N_4) and rGO with a self-snapping mechanism. This hydrogel had great potential as nerve guidance channels (NGCs) (Fig. 7A). The incorporation of rGO into the g-C_3N_4 hydrogel network not only increased the surface charge but also resulted in interesting self-snapping properties that could facilitate the implantation process. The resultant hydrogels exhibited the optimal range of mechanical stiffness for regeneration of peripheral nerve, and hydrogels containing electroactive rGO showed significantly higher neural differentiation compared to their counterparts. In addition, differentiated PC12 cells on the g-C_3N_4H/rGO hydrogel had a neurite length 47% longer than that of the original g-C_3N_4H hydrogel (Fig. 7B). As illustrated in Fig. 7C, they achieved directional properties by introducing sacrificial melt electrowriting (MEW) micro-channels into the hydrogels. Snap NGCs were created using a gradient of crosslinking across the tubular hydrogels, and their study revealed that a length of 10 μm was the most effective in facilitating improved neurite extension. Besides, the hydrogel effectively supports the growth of neural cells and differentiation, demonstrating the significant potential for repairing peripheral nerve injuries (Fig. 7D) [141]. Table 1 provides an overview of the outcomes associated with the application of hydrogel-integrated graphene in the context of neural tissue regeneration.

4.3. Cardiovascular regeneration

The cardiac, the first functional organ to form during embryonic development, is the most critical tissue in the body. Its stylized, four-chambered muscular anatomy is in charge of maintaining constant blood circulation throughout the body. However, regaining functional cardiac tissue is challenging because of the complex hierarchy and cellular diversity composed of smooth muscle cells, endothelial cells (ECs), cardiomyocytes (CMs), fibroblasts, connective tissue cells, immune cells, and other specialized cells [104,142]. The advent of

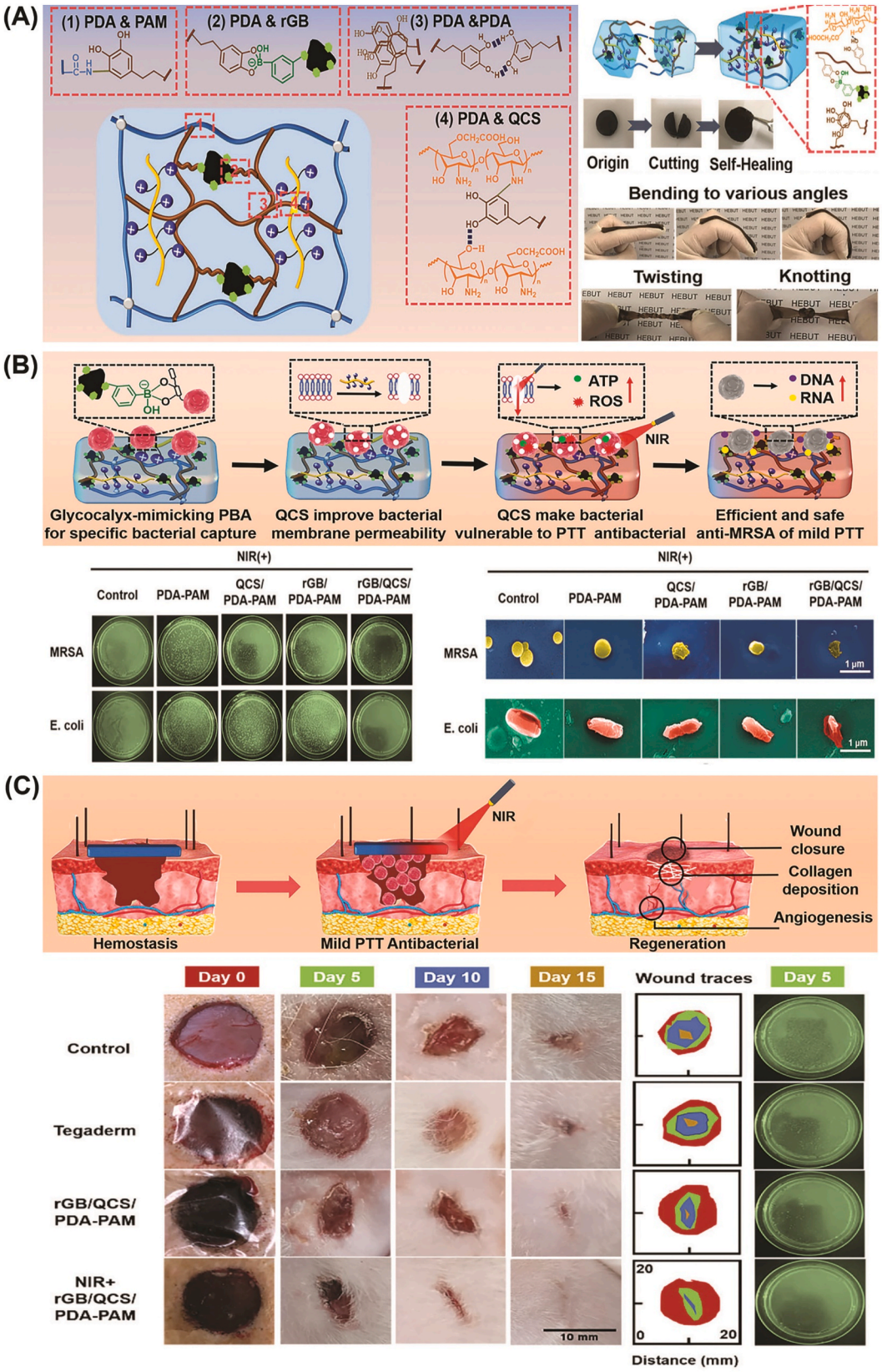

Fig. 6. (A) Illustration of a versatile hydrogel dressing possessing mild photothermal antimicrobial properties (rGB/QCS/PDA-PAM hydrogel) designed to facilitate the healing of methicillin-resistant *S. aureus*-infected wounds at low temperatures. (B) Assessment of the antibacterial performance exhibited by the rGB/QCS/PDA-PAM hydrogel. (C) Representative images and wound profiles were taken at different time points (days 0, 5, 10, and 15) following various treatments. Reproduced with permission from Ref. [133]. Copyright (2023), John Wiley & Sons. (A colour version of this figure can be viewed online.)

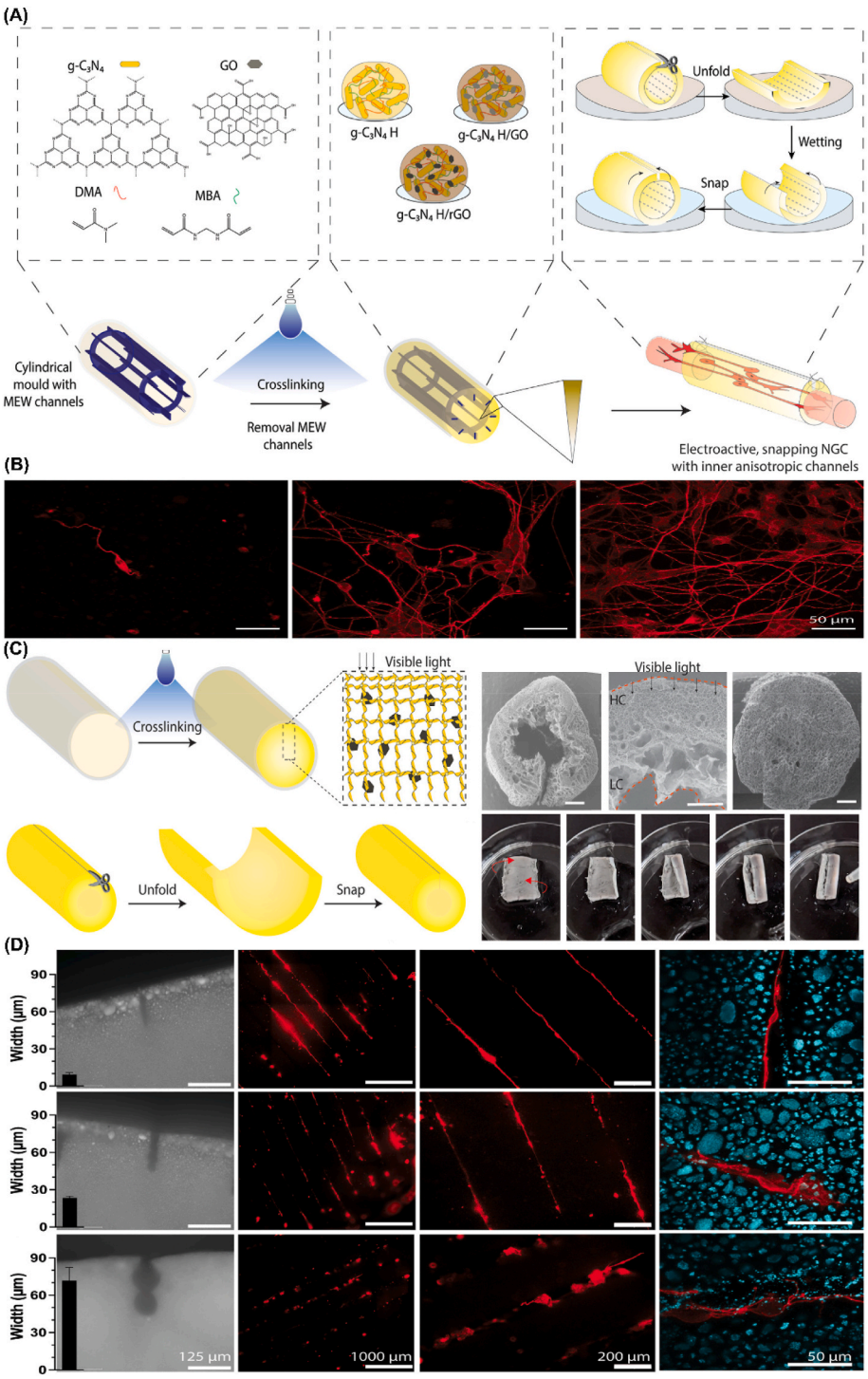

Fig. 7. (A) An illustration of a snapping and anisotropically conductive NGC. DMA and MBA are utilized to produce g-C_3N_4 H through crosslinking activated by blue light. (B) Assessment of PC12 cell differentiation on g-C_3N_4/H. (C) Construction of a nerve guidance hydrogel conduit with snapping capabilities and introduction of inner anisotropic sacrificial channels. (D) Demonstration of the guidance effect achieved by patterned g-C_3N_4 hydrogels. Reproduced with permission from Ref. [141]. Copyright (2022), Elsevier. (A colour version of this figure can be viewed online.)

hydrogels has opened up novel avenues for tackling the difficulties in cardiac tissue engineering. Hydrogels, characterized by their high water content and porous nature, offer the potential to replicate the extracellular matrix and create a structural framework for engineering purposes. Hydrogels provide easy adjustability and offer chemical and physical characteristics, in addition to outstanding biocompatibility and biomanufacturing stability [80,143]. In the field of tissue engineering, conductive hydrogels have found applications in emulating the inherent characteristics of cardiac cell microenvironments. This is because cardiomyocytes and associated progenitor cells exhibit enhanced growth and migration when subjected to electrophysiological stimulation. The necessary conductivity and surface properties are imparted to hydrogel by the incorporation of graphene-based material, further improving the microenvironment of the infarcted area [144,145]. Various examples of hydrogel-integrated graphene in cardiovascular regeneration are shown in Table 1.

To mimic ECM properties, conductive hydrogel design must account for both mechanical strength and electrical activity. In this context, Zhou et al. investigated the integration of GO into OPF hydrogels to enhance mechanical support and improve cellular electrical signaling post-implantation into myocardial infarction sites. Moreover, the introduction of GO into OPF hydrogels exhibited the potential to improve cell attachment *in vitro* settings. When rats were administered an OPF/GO injection four weeks after experiencing a myocardial infarction, there was an observed improvement in Ca^{2+} signal conduction among cardiomyocytes within the infarcted region, in contrast to those treated with phosphate-buffered saline (PBS) or OPF alone [146].

Furthermore, the inclusion of GO enhances the polymeric composite's antioxidant capabilities since sp^2 carbons play a substantial role in neutralizing ROS by creating radical adducts and engaging in electron transfer processes [147]. For example, Yuan et al. engineered a self-healing hydrogel within a silk protein framework, incorporating GO and growth factors, to act as a carrier for cell delivery in regenerative treatment for myocardial infarction (Fig. 8a). As shown in Fig. 8, incorporating GO influenced the structure, leading to a more consistent and finer porous arrangement. This alteration could substantially impact the regulated discharge of growth factors and cell placement. *In vitro* biocompatibility assay for isolating cardiac progenitor cells (CPCs) reveals no negative stimulation and improved cell viability in hydrogels prepared with growth factors, confirming that gel formulations prepared using GO are highly advantageous for implantation for cardiac therapy [148]. Furthermore, oxidative stress and ROS protection analyses demonstrated that prepared gel material had a positive impact and emphasized cardiomyocyte differentiation [149].

A novel injectable gel composed of rGO and alginate was created to transport mesenchymal stem cells (MSCs). The use of microgels containing antioxidant nanomaterials for MSC delivery not only mitigated oxidative stress after myocardial infarction but also augmented the therapeutic effects of the transplanted MSCs. This system, while fostering the regeneration of injured cardiac tissue following a heart attack, provided support for the viability and maturation of CMs [150]. The heart propels blood throughout the body via a highly organized network of blood vessels, which includes arteries, arterioles, and culminates in the capillary system. This intricate, closed-loop structure facilitates the exchange of oxygen, vital nutrients, and metabolic byproducts among various tissues. A variety of intricate synergistic interactions between subendothelial structures, platelets, blood proteins, and plasma coagulation factors form the basis of the human hemostasis system. However, managing these interactions outside of the body can be challenging, especially in emergencies [104,151].

Integrating materials derived from graphene into hydrogels results in the creation of hybrid electroactive scaffolds, which offer enhanced mechanical characteristics, cell adhesion capabilities, and reduced risk of immunogenic responses [152]. Scientific investigations have also revealed that graphene-based materials like surfaces and polymers, possess inherent antibacterial properties [153,154]. Furthermore, components like vascular grafts and heart valves are predominantly exposed to surface shear and tensile stresses induced by the flow of blood. To address this challenge, Ferreira et al. introduced a 4% w/v GO component into a polyethylene glycol (PEG) hydrogel, significantly enhancing the hydrogel's stiffness by 6-fold and its strength by 14-fold. Remarkably, this composite maintained cytocompatibility and preserved its anti-adhesive properties in the presence of endothelial cells, human platelets, and *S. aureus*, at levels comparable to those of pure hydrogels [155].

4.4. Tendon healing

Tendons are fibrous connective tissues responsible for linking muscles to bones. They are primarily composed of organized Col I fibrils, with tenocytes distributed among these Col fibers. Tendons also contain other elements, including various types of Col, proteoglycans, glycoproteins, and elastin. Injuries to tendons can lead to a decrease in their ability to bear loads and compromise their structural integrity. The

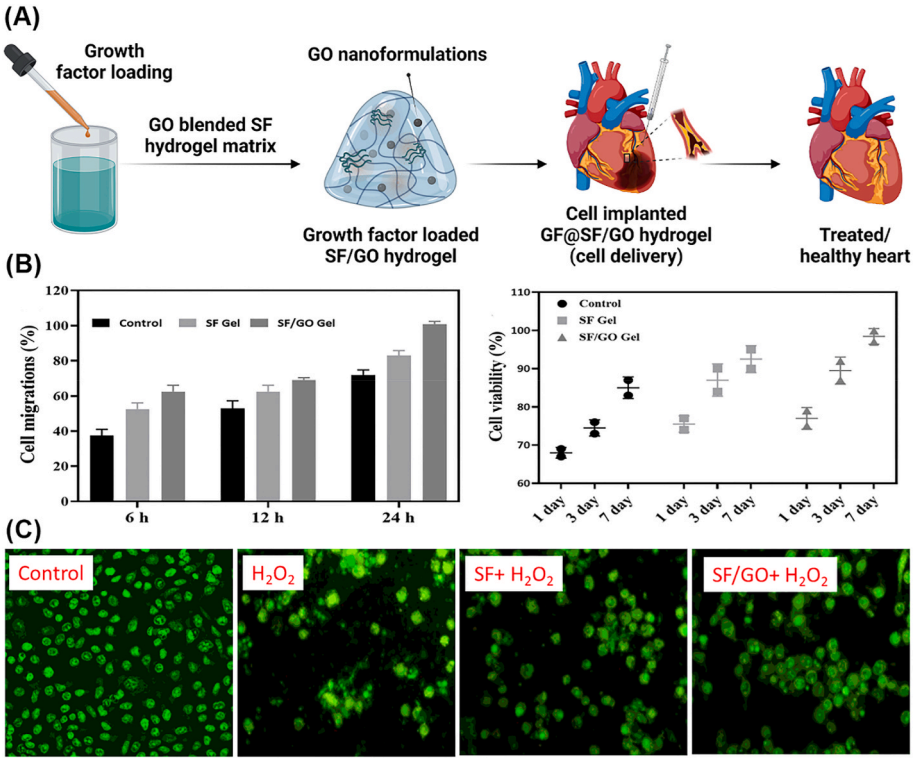

Fig. 8. (A) Schematic represents the proposed structure formation of the hydrogel network with GO nanoformulations and growth factors, along with the site of application for myocardial infarction (MI). (B) Percentage of cell viability on days 1, 3, and 7. (C) TEM image displaying the distribution of GO structure within the SF/GO hydrogel. Reproduced with permission from Ref. [149]. Copyright (2020), Elsevier. (A colour version of this figure can be viewed online.)

treatment of tendon injuries continues to pose difficulties, as existing therapies fall short in completely restoring tendon function following injury, even with the notable progress in tissue engineering for tendon repair. Hydrogels, known for their exceptional biocompatibility and versatility, have gained extensive use and are being explored as promising biomaterial options for tissue regeneration. Functionally tailored hydrogels have been created using a variety of techniques, combining hydrogels with additional elements such as bioactive molecules, medications, or materials to improve tendon repair [156–158]. GO is an advanced material with exceptional properties. It serves as a carrier to facilitate the release of growth factors and drugs. For example, to obtain a sustainable growth factor release system, Bao et al. integrated GO into platelet-rich plasma (PRP). PRP was derived from rabbit whole blood utilizing the double-centrifugation technique. Subsequently, PRP gels incorporating diverse concentrations of GO were formulated to enhance the healing process of traumatic brain injury (TBI) and facilitate supraspinatus tendon reconstruction in a rabbit mode. The hydrogel exhibited outstanding biocompatibility, and the structure of the regenerated tendon tissue closely resembled that of the natural tendon. Moreover, this hydrogel displayed favorable mechanical characteristics and enhanced the proliferation of BMSCs, facilitating both osteogenesis and chondrogenic differentiation, ultimately expediting the reconstruction of the torn supraspinatus tendon [159].

In terms of cell growth and differentiation, Barzegar et al. fortified gelatin hydrogel by combining polyglycerol-functionalized molybdenum disulfide ($PMoS_2$) and polyglycerol (PG)-functionalized rGO. This combination not only enhanced the mechanical characteristics of the hydrogel but also expedited tendon regeneration through the incorporation of PG, while $PMoS_2$ contributed to reducing inflammation during the tendon repair process. Animal studies further confirmed a synergistic effect on the Achilles tendon's functional index, the adhesion scoring system, and the scaffold's ability to regenerate tendons, ultimately leading to improved biomechanical properties in healed tendons [160]. In another study, Yoon et al. introduced a small quantity of GO into alginate, which not only enhanced the scaffold's mechanical properties without inducing cytotoxicity but also promoted the healing of rotator cuff tears [161].

4.5. Skeletal muscle regeneration

Skeletal muscle tissue is composed of contractile muscle cells called myofibers, which have multiple nuclei and account for approximately 30–40% of the body's total weight. These myofibers play a vital role in coordinating movement within the musculoskeletal system and its interaction with the nervous system [162]. While skeletal muscle can recover following an injury, its natural self-regeneration abilities are impaired in cases of chronic damage or severe traumatic injuries. The remarkable mechanical characteristics, excellent electrical conductivity, and flexibility of graphene-based materials with low density render them well-suited as cellular substrates for muscle tissue engineering. These materials have a substantial positive impact on the expansion, attachment, and myogenic differentiation of skeletal muscle cells [116,151]. In a study by Jing et al., the utilization of graphene-based materials within a hydrogel for electroactive tissue engineering applications was explored. They engineered hydrogels composed of CS and GO with properties including adhesion, self-healing, and electrical conductivity. These composite hydrogels exhibited robust mechanical performance, excellent stability, effective adhesion, self-healing capabilities, and rapid recovery, attributes stemming from covalent bonds, supramolecular interactions, hydrogen bonding, and π–π stacking. In addition, the adhesive strength of the composite hydrogel increased by 300%, and its electrical conductivity reached 1.22 mS/cm [163].

For instance, Patel et al. presented innovative fibrous hydrogel films composed of a graphene-polysaccharide nanocomposite, harnessing the combination of graphene's high conductivity and charge carrier mobility with the biocompatibility inherent to polysaccharides. The integration of graphene into these fibrous hydrogel films led to enhancements in tensile strength, electrical conductivity, toughness, and wettability, all while preserving their elasticity. Notably, the presence of these nanocomposite fibrous hydrogel films facilitated the formation of multinucleated myotubes, indicative of myogenesis, when mouse myoblasts were cultured on them. This suggests the considerable potential of this composite as a biomaterial for advancing the regeneration of skeletal muscle tissue [164]. In a distinct investigation, Aparicio-Collado et al. devised novel nanohybrid hydrogels by melding sodium alginate and polycaprolactone (SA/PCL semi-IPN) with calcium ions (Ca^{2+}) serving as crosslinkers for alginate. To overcome the limitations of alginate hydrogels, such as poor cell adhesion and structural stability in water, they introduced conductive rGO nanosheets into the formulation. The incorporation of rGO not only enhanced bioactivity but also prompted improved cellular responses, as shown in Fig. 9A and B. *In vitro* experiments employing C2C12 murine myoblasts demonstrated the non-cytotoxic nature of the conductive nano-hybrid hydrogel, which notably bolstered myoblast adhesion and myogenic differentiation. These findings underscore its potential in regenerating electroactive tissues, particularly within the realm of skeletal muscle tissue engineering (Fig. 9C and D) [165]. Table 2 furnishes a comprehensive summary of the multifaceted applications of hydrogel-integrated graphene in soft tissue engineering and regenerative medicine.

5. Conclusion and future perspectives

Tissue reconstruction surgery contributes to millions of tissue damage, caused by injuries and diseases worldwide annually. In addition to the quality of life, the negative effect of tissue damage on mental health is considerable. Tissue engineering holds the potential to revolutionize treatment repair dysfunctional tissue and extend life expectancy. Tissue engineered alternatives can address a variety of unmet requirements in regenerative medicine. Tissue engineering, a crucial concept involves utilizing biomaterials to facilitate new cell growth and encourage repair. These materials should not only serve as passive spectators but also provide physical scaffolding and behavioral cues for cells. Among numerous types of materials employed in tissue engineering, hydrogels have become one of the most prominent and versatile. These hydrogels can be specifically designed to support cell differentiation, proliferation, and migration. They provide a three-dimensional, highly hydrated environment similar to native soft tissues that allow oxygen and nutrient transport. Crucially, the characteristics of a hydrogel stem from the chemical composition of the base polymer used in its synthesis. The integration of hydrogels with GSSs presents an exclusive array of qualities that can effectively tackle critical issues within the realm of tissue engineering, including mechanical strength, electrical conductivity, and biocompatibility.

Hydrogels combined with graphene-based materials represent a category of 3D biomaterials that hold the promise to transform the landscape of tissue engineering and regenerative medicine. Specifically, their application as a scaffolding environment for cells will undoubtedly lead to many breakthroughs in the engineering of skeletal and electroactive tissues. Moreover, graphene possesses a strong adsorption capacity, making it suitable for delivering genes or drugs due to its unique atomic arrangement. Through the integration of graphene-based materials, it becomes possible to improve the mechanical and surface characteristics of biomaterials. This, in turn, enables the modulation of stem cells' osteogenic, chondrogenic, neurogenic, and cardiomyogenic potentials. Given graphene's demonstrated ability to stimulate stem cell growth and differentiation, these structures may hold potential applications in stem cell-based therapies. In contrast, graphene can undergo alterations with a range of biomolecules, including peptides and proteins, aimed at augmenting its biocompatibility and bioactivity. Such modifications have the potential to amplify the proliferation and functionality of electrically excitable cells, such as cardiomyocytes and neurons. Moreover, they can enhance the acquisition of cellular signals

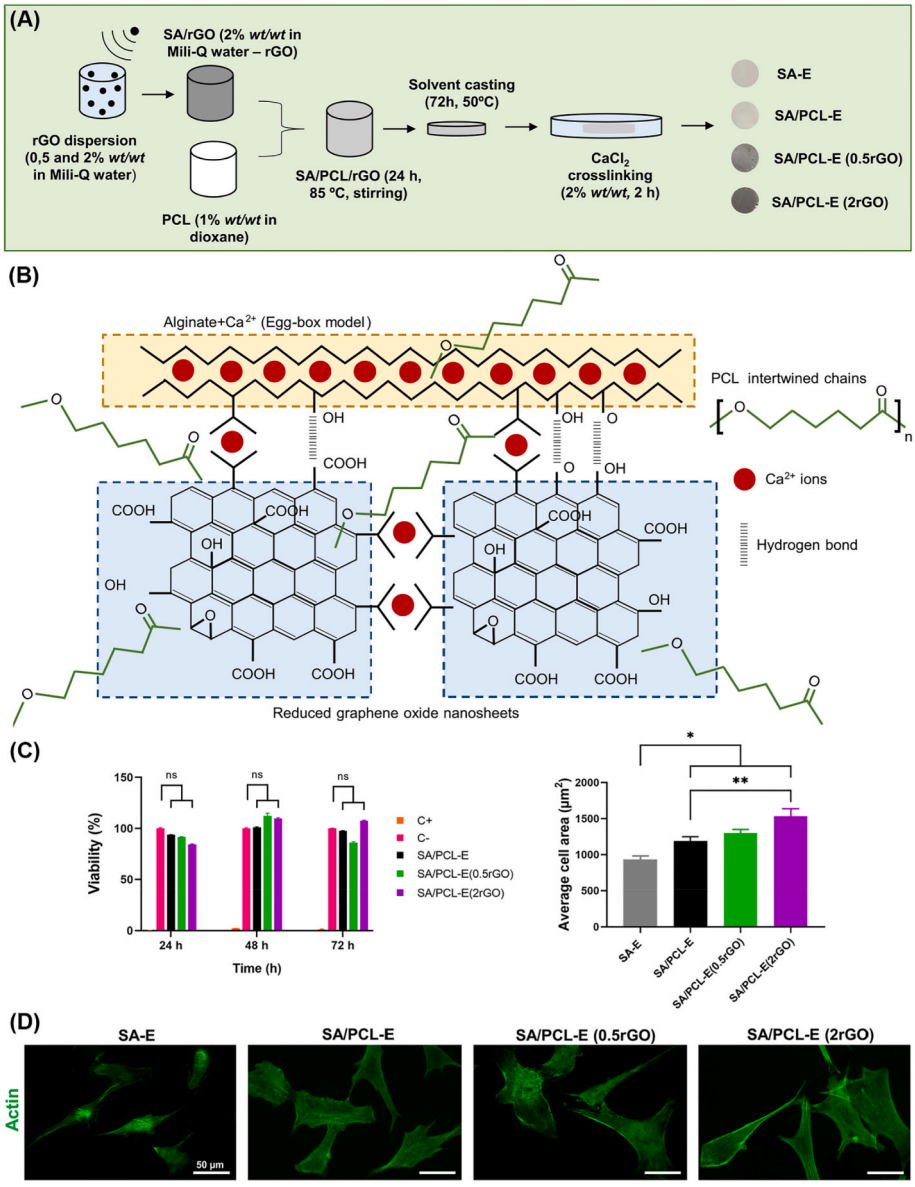

Fig. 9. (A) Schematic represents the process for creating semi-interpenetrating network (IPN) and nanohybrid hydrogels. (B) Schematic depicting the structure of the nanohybrid hydrogel. (C) MTT cytotoxicity results indicate cell viability after 24, 48, and 72 h of exposure to extracts from semi-IPN and nanohybrid hydrogels and average cell adhesion area. (D) Representative immunofluorescence images displaying cells adhered to different hydrogels, visualized through actin staining. Reproduced with permission from Ref. [165]. Copyright (2022), Elsevier. (A colour version of this figure can be viewed online.)

due to graphene's exceptional electrical conductivity. Furthermore, the integration of GSSs within hydrogels holds promise in the realms of biosensors and drug delivery systems [166,167]. The distinctive electrical and mechanical attributes of graphene render it a favorable material for sensing applications and drug transport mechanisms. The incorporation of graphene introduces the potential for improved drug loading and release characteristics, a feature with diverse applications like wound healing and cancer therapy. This capability to manage the precise timing and location of biomolecule release from hydrogels and graphene presents novel prospects for influencing cell responses and tissue regeneration.

From a societal perspective, this research holds the potential to significantly improve the quality of life for individuals dealing with a variety of medical conditions and injuries. For example, hydrogel-integrated GSSs have demonstrated potential in expediting the healing of diabetic ulcers, restoring the functionality of damaged heart tissues following a heart attack, and addressing spinal cord injuries. In addition, the ability to construct intricate 3D structures using these materials could pave the way for the generation of functional organs like the liver, kidney, and lung for transplantation purposes. Moreover, the combination of graphene's chemically adjustable surface with its machinable properties opens avenues for creating complex graphene architectures with diverse applications [168]. Incorporating graphene-based materials into hydrogels, endowed with properties such as wettability or flexibility, makes them promising candidates for producing multifunctional smart materials. This advancement could lead to the development of graphene composites that are responsive to environmental factors or possess characteristics like shape memory or self-folding, thus broadening their biomedical applications.

However, even though graphene-based materials have found extensive application in the field of biomedicine, there exist numerous obstacles that necessitate resolution before these materials can be effectively deployed in clinical contexts. A pivotal issue revolves around the biocompatibility and enduring safety of graphene-based materials.

Table 2
Hydrogel-integrated graphene applications in soft tissue engineering and regenerative medicine.

Application	Type of graphene	Cell line (*in vitro*) or animal models (*in vivo*)	Composition	Preparation	Characterization	Outcomes	Refs.
Skin	rGO	RBC & L929/ mouse	QCS−CD−AD & QCS−CD−AD/ GO	Mixing/host-guest interaction	^{1}H NMR, FTIR, SEM, rheological measurements, conductivity test, swelling, adhesive strength test, degradation test, heat maps, self-healing study, antibacterial study, hemolysis ratio, proliferation study, live/ dead staining, histological analysis, immunofluorescence staining	• Favorable mechanical stability, adequate conductivity, strong biocompatibility, swift self-healing capacity, photo-thermal characteristics, and antibacterial effects triggered by NIR radiation • Considerable enhancement of *in vivo* wound healing, marked by increased epidermal and granulation tissue thickness, expanded Col area coverage, and elevated VEGF expression	[42]
	rGO	NHDF	PCL−CA/ CS−rGO	Blending	NIR, SEM, ATR-FTIR, swelling behavior, WCA, MTS assay, CLSM, and antibacterial study	• Production of NIR-responsive wound dressing by a combi-nation of CS_rGO hydrogel and an electrospun PCL_CA membrane • Increase the NIR absorption capacity by incorporating rGO • Improve antibacterial properties • Support cell adhesion and growth	[186]
	rGO	N.A.	PC/rGO/PVA	Blending/ crosslinking	XPS, FE-SEM, rheological test, oscillatory frequency sweeps, mechanical tests, LCR, self-healing study, adhesive strength study, ECG and EMG signals study	• Excellent stretchability, compliance, and self-healing ability • Exceptional wearability and sensitivity to strain, resembling and detecting real skin epidermal movements effectively • Suitable for use as an adhesive electrode for precise capturing of ECG and EMG signals • Replicate the tactile capabilities of natural skin via a hierarchical hydrogel network design	[187]
	Graphene, GO	NIH 3T3	PVA/GBM/Av	Freeze-thawing	SEM, FTIR, Raman, contact angle, electrical conductivity test, tensile test, degradation test, antibacterial assay, cell cytotoxicity assay	• Good stability, excellent hydrophilicity, mechanical properties, and electrical conductivity comparable to human skin tissue • Antibacterial and non-cytotoxic properties confirm its potential as a wound dressing	[188]
	GO	HaCaT/mouse	IFI6-PDA−GO/ SA	Blending	FTIR, XPS, SEM, EDS, DLS & zeta potential, SDS–PAGE protein analysis, FITC/DAPI staining, antibacterial study, CCK-8 assay, flow cytometry, *in vitro* tube formation assay, *in vitro* cytological study, western blot, cell clone formation assay, HE staining, immunohistochemistry staining, real-time PCR, and ROS measurements	• Excellent antibacterial activity, and biocompatibility • Facilitate cell proliferation, migration, and vascularization, while also modulating the immune microenvironment • Enhance the resolution of inflammation in RISI wounds, leading to increased granulation tissue formation, angiogenesis, and Col deposition	[189]
	Graphene	Mice	NAGA/ graphene	Photopolymerization	Self-healing performance study, photothermal capacity, antibacterial study, H&E-staining, Masson's trichrome staining, and immunohistochemical	• High tensile strength, good stretchability, and self-recoverability • Great photothermal transition activity • Excellent antibacterial activity	[190]

(*continued on next page*)

Table 2 (*continued*)

Application	Type of graphene	Cell line (*in vitro*) or animal models (*in vivo*)	Composition	Preparation	Characterization	Outcomes	Refs.
						• Efficiently expedite wound healing by eradicating microorganisms and facilitating Col deposition and angiogenesis	
Neural	GO	NE-4C, ATCC, CRL-2925 and SH-SY5Y, ATCC, CRL-2266/male C57BL/6 N mice	MoS_2/GO/PVA	Freezing- thawing	HRTEM, SEM, Raman spectra, elastic modulus, conductivity, swelling ratio, XRD, FTIR, zeta potential, cytotoxicity study, live/dead staining, hemolysis tests, cell differentiation study, immunostaining fluorescence, gene expression analysis, ROS detecting, flow cytometry, histological staining, immunohistochemistry staining, functional assessment, and western blot	• Promote NE-4C to neuronal differentiation • Inhibit the development of astrocytes • Excellent anti-oxidative properties • Facilitate the regeneration of spinal cord tissue • Enhance the mobility of mice with SCIs	[191]
	Graphene	RSC96, HUVECs/ male Sprague-Dawley rats	Netrin-1-loaded GMT/DN	Blending	FTIR, optical image, SEM, Raman spectrum, stress−strain behavior, transwell migration assay, H&E and Masson staining, immunofluorescent staining	• The GMT/DN hydrogel aids in the growth and orientation of RSC96 • neural cells • Netrin-1 facilitates the movement of Schwann cells • Promote angiogenesis • Promote regeneration of peripheral nerve • Restoration of the denervated muscle	[192]
	Graphene	N27s	Graphene & cells−alginate	Microfibrous/ microfluidic	SEM, porosity study, conductivity, and live/dead assay	• Embedding rat neural cells in conductive 3D tissue scaffolds • Increase electrical conductivity • Promoting cell migration beyond the fiber boundaries	[193]
	GO	PC12/male pathogen-free C57BL/6 mice	CFGO	Blending	FTIR, UV–Vis, XPS, TEM, rheological study, MTT assay, neurite outgrowth assay, live/ dead cells assay, F-actin staining, western blot, and immunochemistry staining	• Facilitating neurite outgrowth, stabilizing microtubule networks, and increasing the expression of essential neural markers • Great potential for nerve regeneration. • Facilitate rapid brain recovery • Markedly elevating reactive astrocyte levels in the hippocampal DG region • Greater ability to maintain cholinergic balance by locally releasing acetylcholine	[194]
	GO	Schwann/male wistar rats	NH_2-GO/ Fr−Col−CS	Blending	Eye closure and whisker function test, luxol fast blue staining, histological examination, and immunostaining	• Increase the number of regenerating axons and mean axon diameter • significant neuroregenerative properties	[195]
	GO	Schwann/rats	PAM/GO/gel/ SA	Blending/molding	SEM, swelling ratio, mechanical properties, HE staining, Masson trichrome staining, and immunofluorescence histochemical staining	• Good flexibility, bioactivity, and stability • Suitable mechanical properties • Promote the repair of rat sciatic nerve injury	[196]
Cardiovascular	rGO	hBM-MSCs	ALG−rGO	Crosslinking	FTIR, rheological study, SEM, swelling ratio, conductivity study, MTT assay, AO/PI staining, and qRT-PCR	• Enhance cell–cell interactions and offer a suitable platform for upregulating cardiomyocyte gene expression, even without electrical stimulation	[197]
	rGO	H9c2(2-1) & ATCC/C57BL/6J rats	PANI −rGO/ Mxenes	Blending/ crosslinking	SEM, EDS, XRD, mechanical properties, degradation study, CCK-8 assayImmunostaining, H&E staining, and MTC staining	• Biocompatible, wet-adhesive, stretchable, lightweight, thin-layer, and flexible • High areal capacitance and energy density	[198]

(*continued on next page*)

Table 2 (*continued*)

Application	Type of graphene	Cell line (*in vitro*) or animal models (*in vivo*)	Composition	Preparation	Characterization	Outcomes	Refs.
	CNTs, GO, rGO	hiPSC-cardiomyocytes	CNT−GelMA, GO−GelMA, rGO−GelMA	Blending/ crosslinking	XPS, TEM, AFM, SEM, porosity study, MTS assay, immunofluorescence image, immunostaining, F-actin staining, electrophysiological properties, conductivity study, beating frequency, gene expression analysis, qRT-PCR	• Atraumatic to cardiomyocytes and mice • Exhibit good electrical conductivity, a native ECM-like nanofibrous structure with improved local mechanical properties • Promote the mature morphology of cardiomyocytes, ensuring their viability, and increasing the expression of functional cardiac markers • Increase mechanosensory expression, leading to more robust contractions • Generate distinct cardiomyocyte phenotypes and varying levels of maturity based on the substrate (CNT-GelMA: ventricular-like, GO-GelMA: atrial-like, and rGO-GelMA: ventricular/atrial mixed phenotypes)	[199]
	rGO	hiPSC-CMs & HS-27A	dECM/rGO	Crosslinking/ bioprinting	LC/MS analysis, SEM, mechanical and electrical properties, contractile function study, RT-qPCR analysis, gene expression analysis, fluorescent image, sarcomere study, and patch clamp measurements	• Significant increase in twitch force and increased expression of genes that regulate contractile function • Improve electrophysiological function • Can be used as a bioink for high-throughput cardiac tissue printing	[200]
	GQDs	HCAECs	hMSCs –CS/CG & CS/ CG−GQDs	Lyophilization	TEM, UV-PL, FTIR, XRD, TGA, SEM, MTT assay, live/dead assay, *in vitro* gene expressions, echocardiography analysis, MTS staining, immunohistochemical staining	• Improve cell survival rate • Increase expression of pro-inflammatory factors • Improve pro-angiogenic factors and early cardiogenic markers • Enhance vessel density activities • Increase ejection fraction with reduced infarct size at the MI heart site	[201]
Skeletal Muscle	GO	C2C12	GO/PAAm	Blending/FLA	SEM, cross-sectional analysis, mechanical and electrical study, EIS, immunostaining, qRT-PCR, H&E staining	• Promote myoblasts differentiation and alignment • Good tissue compatibility • Desirable conductivity for delivering electrical signals	[202]
	GO	C2C12	PEGDA/ MAETAC/ PEDOT:PSS/GO	Crosslinking/ molding	Contact angle, EIS, XPS, and cell viability assay	• Enhancing mobility and stability through the incorporation of conductive polymers in the outer layer • Utilizing gentle electrical stimulation leads to increased cell viability and stronger contractile force • Provide both electrical and mechanical stimulation	[203]

Although graphene has exhibited biocompatibility in preliminary *in vitro* and *in vivo* investigations [154], additional comprehensive research is imperative to fathom its protracted implications and ascertain any latent toxicity concerns. In response to the biocompatibility issues, there has been considerable focus on surface modifications, including the functionalization with proteins or cytokines [169,170]. It is prudent to advance the development of testing models aimed at gaining a more profound understanding of the cytotoxicity mechanisms associated with graphene-based materials, prior to their prospective clinical application. Another challenge is the optimization of the fabrication techniques and protocols for controlling the properties of the hydrogel-integrated GSSs. For instance, fabrication based on physically cross-linked methods limits functional and mechanical properties, or the addition of chemical cross-linkers produces poor absorption properties and cross-linking reaction depends on the mixing process. Moreover, *in situ* polymerization faces the challenges of increasing post-tensile strength and easily breaks at low deformation at elongation. Furthermore, the addition of metal ions or hydrophobic monomers shows an increase in the fracture stress of the composite with increasing GO concentration [171]. Further research in this field should focus on addressing these challenges and

exploring new applications for these materials. For example, investigating the interactions between the hydrogel-integrated GSSs and the immune system may provide insights into the biocompatibility and immunomodulatory properties of these materials. Further investigations may delve into the application of these substances in drug transport, cancer treatment, and biological sensing. In general, the prospects for hydrogel-integrated GSSs in tissue engineering and regenerative medicine hold great promise, and significant advancements are anticipated in the near future.

CRediT authorship contribution statement

Iman Zare: Writing – original draft. **Mojdeh Mirshafiei:** Writing – original draft. **Bahareh Kheilnezhad:** Writing – original draft. **Bahareh Farasati Far:** Writing – original draft. **Mahnaz Hassanpour:** Writing – original draft. **Esmail Pishbin:** Writing – original draft. **Shahrzad Sadat Eftekhar Vaghefi:** Writing – original draft. **Fatemeh Yazdian:** Writing – original draft. **Hamid Rashedi:** Writing – original draft. **Anwarul Hasan:** Writing – original draft. **Xiangdong Wang:** Writing – original draft. **Mohsen Adeli:** Writing – review & editing, Conceptualization. **Pooyan Makvandi:** Writing – review & editing, Conceptualization.

Declaration of competing interest

The authors declare that they have no known competing financial interests or personal relationships that could have appeared to influence the work reported in this paper.

Data availability

No data was used for the research described in the article.

Acknowledgements

A Hasan acknowledges the partial financial support from the grant NPRP12S-0310-190276 from the Qatar National Research Fund (a member of The Qatar Foundation). The statements herein are the sole responsibilities of authors.

Abbreviation

Alg	alginate
ALP	alkaline phosphatase
DAPI	2-(4-amidinophenyl)-6-indolecarbamidine dihydrochloride
a-PVA	annealed PVA
AFM	atomic force microscopy
ATR-FTIR	attenuated total reflectance-fourier transform infrared spectroscopy
BMSCs	bone marrow-derived mesenchymal stem cells
CNTs	carbon nanotubes
CNTpega	carbon nanotube poly (ethylene glycol) acrylate
CPCs	cardiac progenitor cells
CMs	cardiomyocytes
CA	cellulose acetate
CNS	central nervous system
CS	chitosan
Col	collagen
CLSM	confocal laser scanning microscopy
dECM	decellularized porcine myocardial extracellular matrix
DLS	dynamic light scattering
EIS	electrochemical impedance spectroscopy
ECG	electrocardiograph
EMG	electromyography
EDS	energy dispersive spectroscopy
ECs	endothelial cells
ECM	extracellular matrix
FE-SEM	field-emission scanning electron microscopy
FLA	femtosecond laser ablation
FEA	finite element analysis
FITC	fluorescein isothiocyanate
FTIR	Fourier transform infrared
GEH	graphene elastic hydrogel
GO	graphene oxide
GOa	graphene oxide acrylate
GQDs	graphene quantum dots
g-C_3N_4	graphitic carbon nitride
HREM	high resolution electron microscopy
hiPSCs	human induced pluripotent stem cells
hDPSCs	human dental pulp stem cells
HA	hydroxyapatite
IFI6	interferon-α inducible protein 6
IPN	interpenetrating network
LC-MS	liquid chromatography tandem mass spectrometry
MSCs	mesenchymal stem cells
GelMA	methacrylate gelatin
MEW	melt electrowriting
MRSA	methicillin-resistant *Staphylococcus aureus*
MI	myocardial infarction
NIR	near-infrared
NGCs	nerve guidance channels
NS/PC	neural stem/precursor cells
OPF	oligo (polyethylene glycol fumarate)
OCN	osteocalcin
PCG	peptide-coated graphene
PNS	peripheral nervous system
PDL	periodontal ligament
rGB	phenylboronic acid-functionalized graphene
PBS	phosphate-buffered saline
PTT	photothermal therapy
PRP	platelet-rich plasma
PAM	polyacrylamide
PCL	polycaprolactone
PEDOT	poly(3,4-ethylenedioxythiophene)
PANI	polyaniline
PCL	polycaprolactone
PGO	polydopamine-mediated graphene oxide
PEG	polyethylene glycol
PEGDA	poly(ethylene glycol) diacrylate
PG	polyglycerol
PPy	polypyrrole
PSS	poly (4-styrene sulfonate)
PVA	polyvinyl alcohol
PPR	pseudopolyrotaxane
PDA	polydopamine
PDLSCs	periodontal ligament stem cell
PNIPAAm	poly (N-isopropylacrylamide)
QAS	quaternary ammonium salts
QCS	quaternary chitosan
RISI	radiation-induced skin injury
rBMSCs	rat BMSCs
rGO	reduced graphene oxide
ROS	reactive oxygen species
SEM	scanning electron microscopy
Ser	sericin
SF	silk fibroin
SCIs	spinal cord injuries
SA	sodium alginate
TMJ	temporomandibular joint
TEOS	tetraethyl orthosilicate
3D	three dimensional
TEM	transmission electron microscopy
WCA	water contact angle

XRD X-ray diffraction
XPS X-ray photoelectron spectroscopy

Appendix A. Supplementary data

Supplementary data to this article can be found online at https://doi.org/10.1016/j.carbon.2024.118970.

References

[1] K.D. Nordham, S. Ninokawa, The history of organ transplantation, in: Baylor University Medical Center Proceedings, Taylor & Francis, 2022.
[2] S.Y.Z. Moghaddam, et al., Tannic acid as a green crosslinker for biomaterials applications, Mini Rev. Med. Chem. 23 (2023) 1320–1340.
[3] B. Kheilnezhad, et al., An overview of polyaniline in tissue engineering, Tissues and materials 3 (4) (2020) 6–22.
[4] P. Pires, F. Damiri, E.N. Zare, A. Hasan, R.E. Neisiany, F. Veiga, P. Makvandi, A. C. Paiva-Santos, A review on natural biopolymers in external drug delivery systems for wound healing and atopic dermatitis, Int. J. Biol. Macromol. 263 (2024) 130296.
[5] F.D. Moghaddam, G. Heidari, E.N. Zare, E. Djatoubai, A.C. Paiva-Santos, F. R. Bertani, A. Wu, Carbohydrate polymer-based nanocomposites for breast cancer treatment, Carbohydr. Polym. 304 (2023) 120510.
[6] N. Biglari, E.N. Zare, Conjugated polymer-based composite scaffolds for tissue engineering and regenerative medicine, Alex. Eng. J. 87 (2024) 277–299.
[7] B. Kheilnezhad, A.J.B.S. Hadjizadeh, A review: progress in preventing tissue adhesions from a biomaterial perspective, Biomater. Sci. 9 (8) (2021) 2850–2873.
[8] C.M. Tringides, et al., Tunable conductive hydrogel scaffolds for neural cell differentiation, Adv. Healthcare Mater. 12 (7) (2023) 2202221.
[9] R.M. Staruch, et al., Injectable pore-forming hydrogel scaffolds for complex wound tissue engineering: designing and controlling their porosity and mechanical properties, Tissue Eng. B Rev. 23 (2) (2017) 183–198.
[10] H. Lu, et al., Applications of graphene-based composite hydrogels: a review, RSC Adv. 7 (80) (2017) 51008–51020.
[11] L.M.T. Phan, et al., Graphene integrated hydrogels based biomaterials in photothermal biomedicine, Nanomaterials 11 (4) (2021) 906.
[12] C.D.J.P.C. Spicer, Hydrogel scaffolds for tissue engineering: the importance of polymer choice, Polym. Chem. 11 (2) (2020) 184–219.
[13] F. Aavani, et al., 3D bio-printing for skin tissue regeneration: Hopes and Hurdles, Curr. Stem Cell Res. Ther. 17 (5) (2022) 415–439.
[14] A. Esmaeili, et al., Acellular fish skin for wound healing, Int. Wound J. 20 (2023) 2924–2941.
[15] H. Chavda, C.J. Patel, Effect of crosslinker concentration on characteristics of superporous hydrogel, Int. J. Pharm. Investig 1 (1) (2011) 17–21.
[16] R. Eivazzadeh-Keihan, et al., Effects of mechanical properties of carbon-based nanocomposites on scaffolds for tissue engineering applications: a comprehensive review, Nanoscale Adv. 6 (2024) 337–366.
[17] R.G. Bai, et al., Graphene: a versatile platform for nanotheranostics and tissue engineering, Prog. Mater. Sci. 91 (2018) 24–69.
[18] M. Adel, et al., Nanodiamonds for tissue engineering and regeneration, J. Drug Deliv. Sci. Technol. 90 (2023) 105130.
[19] K. Huang, et al., MMP9-Responsive graphene oxide quantum dot-based nano-in-micro drug delivery system for combinatorial therapy of choroidal neovascularization, Small (2023) 2207335.
[20] S.K. Krishnan, et al., Graphene-based field-effect transistors in biosensing and neural interfacing applications: recent advances and prospects, Anal. Chem. 95 (5) (2023) 2590–2622.
[21] H. Yan, et al., Planted graphene quantum dots for targeted, enhanced tumor imaging and long-term visualization of local pharmacokinetics, Adv. Mater. (2023) 2210809.
[22] S. Pilato, et al., 3D graphene oxide-polyethylenimine scaffolds for cardiac tissue engineering, ACS Appl. Mater. Interfaces 15 (2023) 14077–14088.
[23] M.A. Mostafavi, A.J.M.S. Mouradzadegun, E. B, Reinforced polymeric nanocomposites of the Amino-Decorated Polycalix [4] resorcinarene with graphene oxide and reduced graphene oxide as promising candidates in materials science, Mater. Sci. Eng., B 271 (2021) 115273.
[24] A. Boddu, et al., ROS-generating, pH-responsive and highly tunable reduced graphene oxide-embedded microbeads showing intrinsic anticancer properties and multi-drug co-delivery capacity for combination cancer therapy, Drug Deliv. 29 (1) (2022) 2481–2490.
[25] X.-M. Huang, et al., Physical properties and device applications of graphene oxide, Frontiers of Physics 15 (2020) 1–70.
[26] G. Liao, et al., Preparation, properties, and applications of graphene-based hydrogels, Front. Chem. 6 (2018) 450.
[27] C. Martín, et al., Graphene improves the biocompatibility of polyacrylamide hydrogels: 3D polymeric scaffolds for neuronal growth, Sci. Rep. 7 (1) (2017) 10942.
[28] R. Geetha Bai, et al., Graphene-based 3D scaffolds in tissue engineering: fabrication, applications, and future scope in liver tissue engineering, Int. J. Nanomed. (2019) 5753–5783.
[29] J. Sturala, et al., Chemistry of graphene derivatives: synthesis, applications, and perspectives, Chem.–Eur. J. 24 (23) (2018) 5992–6006.
[30] P. Sun, Q.J.M.M. Li, Engineering, *Tension-Responsive Graphene Oxide Conductive Hydrogel With Robust Mechanical Properties And High Sensitivity For Human Motion Monitoring*, Macromolecular Materials and Engineering, 2022 2200529.
[31] S. Bashir, et al., Conducting polymer/graphene hydrogel electrodes based aqueous smart Supercapacitors: a review and future prospects, J. Electroanal. Chem. 898 (2021) 115626.
[32] S. Parvaneh, et al., Carboxymethyl cellulose/starch/reduced graphene oxide composite as a pH-sensitive nanocarrier for curcumin drug delivery, Int. J. Biol. Macromol. (2023) 124566.
[33] A.P. Najafabadi, et al., pH-sensitive ameliorated quercetin delivery using graphene oxide nanocarriers coated with potential anticancer gelatin-polyvinylpyrrolidone nanoemulsion with bitter almond oil, J. Drug Deliv. Sci. Technol. 82 (2023) 104339.
[34] I.E. Souza, et al., Short review on the use of graphene as a biomaterial–PROSPECTS, and CHALLENGES in Brazil, J. Mater. Res. Technol. 19 (2022) 2410–2430.
[35] J. Li, et al., Promising graphene-based nanomaterials and their biomedical applications and potential risks: a comprehensive review, ACS Biomater. Sci. Eng. 7 (12) (2021) 5363–5396.
[36] H. Zhao, et al., Graphene-based nanomaterials for drug and/or gene delivery, bioimaging, and tissue engineering, Drug Discov. Today 22 (9) (2017) 1302–1317.
[37] J. Sengupta, Carbon nanotube fabrication at industrial scale: opportunities and challenges, Handbook of nanomaterials for industrial applications (2018) 172–194.
[38] O.C. Compton, S.T. Nguyen, Graphene oxide, highly reduced graphene oxide, and graphene: versatile building blocks for carbon-based materials, Small 6 (6) (2010) 711–723.
[39] C. Chen, Y. Xi, Y.J.M. Weng, Progress in the development of graphene-based biomaterials for tissue engineering and regeneration, Materials 15 (6) (2022) 2164.
[40] S. Kumar, S.H.J.C.C. Parekh, Linking graphene-based material physicochemical properties with molecular adsorption, structure and cell fate, Commun. Chem. 3 (1) (2020) 8.
[41] D. Ege, A.R. Kamali, A.R. Boccaccini, Graphene oxide/polymer-based biomaterials, Adv. Eng. Mater. 19 (12) (2017) 1700627.
[42] B. Zhang, et al., Injectable self-healing supramolecular hydrogels with conductivity and photo-thermal antibacterial activity to enhance complete skin regeneration, Chem. Eng. J. 400 (2020) 125994.
[43] S.-R. Ignat, et al., Versatile biomaterial platform enriched with graphene oxide and carbon nanotubes for multiple tissue engineering applications, Int. J. Mol. Sci. 20 (16) (2019) 3868.
[44] F. Mouhat, F.-X. Coudert, M.-L.J.N.c. Bocquet, Structure and chemistry of graphene oxide in liquid water from first principles, Nat. Commun. 11 (1) (2020) 1566.
[45] J. Yi, et al., Graphene oxide-incorporated hydrogels for biomedical applications, Polym. J. 52 (8) (2020) 823–837.
[46] M.K. Satapathy, et al., Microplasma-assisted hydrogel fabrication: a novel method for gelatin-graphene oxide nano composite hydrogel synthesis for biomedical application, PeerJ 5 (2017) e3498.
[47] P. Passaretti, Graphene oxide and biomolecules for the production of functional 3D graphene-based materials, Front. Mol. Biosci. 9 (2022) 774097.
[48] X. Hu, D. Li, L.J.E.S.N. Mu, Biotransformation of graphene oxide nanosheets in blood plasma affects their interactions with cells, Environ. Sci.: Nano 4 (7) (2017) 1569–1578.
[49] Y. Qi, et al., The biotransformation of graphene oxide in lung fluids significantly alters its inherent properties and bioactivities toward immune cells, NPG Asia Mater. 10 (5) (2018) 385–396.
[50] W. Yang, et al., The physicochemical properties of graphene nanocomposites influence the anticancer effect, Journal of Oncology 2019 (2019).
[51] Y. Chen, T. Szkopek, M.J.M.H. Cerruti, Supramolecular temperature responsive assembly of polydopamine reduced graphene oxide, Mater. Horiz. 10 (2023) 2638–2648.
[52] Y. Xiao, et al., Few-layered Ti3C2TX coupled with Fe3O4 nanoparticles assembled in reduced graphene oxide hydrogel as advanced electrodes for high-energy supercapcitor, New J. Chem. 47 (2023) 2575–2584.
[53] U.N. Maiti, et al., Three-dimensional shape engineered, interfacial gelation of reduced graphene oxide for high rate, large capacity supercapacitors, Adv. Mater. 26 (4) (2014) 615–619.
[54] S.K. Singh, et al., Thrombus inducing property of atomically thin graphene oxide sheets, ACS Nano 5 (6) (2011) 4987–4996.
[55] M.F. Graça, et al., Reduced graphene oxide-enriched chitosan hydrogel/cellulose acetate-based nanofibers application in mild hyperthermia and skin regeneration, Int. J. Biol. Macromol. 229 (2023) 224–235.
[56] S.R. ur Rehman, et al., Reduced graphene oxide incorporated GelMA hydrogel promotes angiogenesis for wound healing applications [corrigendum], Int. J. Nanomed. 17 (2022) 2643–2645.
[57] K. Soleimani, et al., Bioconjugated graphene oxide hydrogel as an effective adsorbent for cationic dyes removal, Ecotoxicol. Environ. Saf. 147 (2018) 34–42.
[58] S.A. Malik, et al., Modulation of protein–graphene oxide interactions with varying degrees of oxidation, Nanoscale Adv. 2 (5) (2020) 1904–1912.
[59] K. Chaudhary, et al., Protein immobilization on graphene oxide or reduced graphene oxide surface and their applications: influence over activity, structural and thermal stability of protein, Adv. Colloid Interface Sci. 289 (2021) 102367.
[60] E.I. Biru, et al., Graphene oxide–protein-based scaffolds for tissue engineering: recent advances and applications, Polymers 14 (5) (2022) 1032.

[61] C. McCallion, et al., Graphene in therapeutics delivery: problems, solutions and future opportunities, Eur. J. Pharm. Biopharm. 104 (2016) 235–250.
[62] M. Zhang, et al., Dual-crosslinked hyaluronic acid hydrogel with self-healing capacity and enhanced mechanical properties, Carbohydr. Polym. 301 (2023) 120372.
[63] S. Tang, Z. Liu, X.J.C.L. Xiang, Graphene oxide composite hydrogels for wearable devices, Carbon Letters 32 (6) (2022) 1395–1410.
[64] C. Cha, et al., Controlling mechanical properties of cell-laden hydrogels by covalent incorporation of graphene oxide, Small 10 (3) (2014) 514–523.
[65] C. Wan, M. Frydrych, B.J.S.M. Chen, Strong and bioactive gelatin–graphene oxide nanocomposites, Soft Matter 7 (13) (2011) 6159–6166.
[66] R. Kurapati, et al., Biodegradation of graphene materials catalyzed by human eosinophil peroxidase, Faraday discussions 227 (2021) 189–203.
[67] L. Newman, et al., Hypochlorite degrades 2D graphene oxide sheets faster than 1D oxidised carbon nanotubes and nanohorns, npj 2D Materials and Applications 1 (1) (2017) 39.
[68] R. Tarcan, et al., Reduced graphene oxide today, J. Mater. Chem. C 8 (4) (2020) 1198–1224.
[69] E. Díaz, A. Mendivil, J.J.B. León, Crystallization behavior and morphology of biodegradable poly (ε-caprolactone)/Reduced graphene oxide scaffolds, Biomimetics 7 (3) (2022) 116.
[70] M. Gautam, S. Kanade, B.B. Kale, Electrochemical energy storage and conversion applications of graphene oxide: a review, Energy & Fuels 37 (22) (2023) 17134–17160.
[71] S. Vijayavenkataraman, et al., 3D-printed PCL/rGO conductive scaffolds for peripheral nerve injury repair, Artif. Organs 43 (5) (2019) 515–523.
[72] X. Zhao, et al., Biomimetic, highly elastic conductive and hemostatic gelatin/rGO-based nanocomposite cryogel to improve 3D myogenic differentiation and guide in vivo skeletal muscle regeneration, Appl. Mater. Today 26 (2022) 101365.
[73] Y. Tan, et al., Engineering a conduction-consistent cardiac patch with rGO/PLCL electrospun nanofibrous membranes and human iPSC-derived cardiomyocytes, Front. Bioeng. Biotechnol. (2023) 11.
[74] F. Cheng, et al., The Fabrication of Conductive Materials-Decorated Hydrogel for Tissue Repair, Molecular Systems Design & Engineering, 2023.
[75] A. Magaz, et al., Graphene oxide and electroactive reduced graphene oxide-based composite fibrous scaffolds for engineering excitable nerve tissue, Mater. Sci. Eng. C 119 (2021) 111632.
[76] J. Niple, et al., A portable meter for measuring low frequency currents in the human body, The European Bioelectromagnetics Association 25 (5) (2004) 369–373.
[77] Y. Wu, et al., Electroactive biodegradable polyurethane significantly enhanced Schwann cells myelin gene expression and neurotrophin secretion for peripheral nerve tissue engineering, Biomater. Sci. 87 (2016) 18–31.
[78] Y. Liang, et al., Self-healing, self-adhesive and stable organohydrogel-based stretchable oxygen sensor with high performance at room temperature, Nano-Micro Lett. 14 (1) (2022) 52.
[79] D. Trucco, et al., Graphene oxide-doped gellan gum–PEGDA bilayered hydrogel mimicking the mechanical and lubrication properties of articular cartilage, Adv. Healthcare Mater. 10 (7) (2021) 2001434.
[80] S.B. Ryu, K.M. Park, K.D. Park, In situ graphene oxide-gelatin hydrogels with enhanced mechanical property for tissue adhesive and regeneration, Biochem. Biophys. Res. Commun. 592 (2022) 24–30.
[81] C.M. Tringides, et al., Tunable conductive hydrogel scaffolds for neural cell differentiation, Adv. Healthcare Mater. 12 (7) (2023) 2202221.
[82] J. Ruhkopf, et al., Role of substrate surface morphology on the performance of graphene inks for flexible electronics, ACS Appl. Electron. Mater. 1 (9) (2019) 1909–1916.
[83] T.S. Tran, N.K. Dutta, N.R. Choudhury, Graphene inks for printed flexible electronics: graphene dispersions, ink formulations, printing techniques and applications, Adv. Colloid Interface Sci. 261 (2018) 41–61.
[84] A.I. Cernencu, et al., 3D double-reinforced graphene oxide–nanocellulose biomaterial inks for tissue engineered constructs, RSC Adv. 13 (34) (2023) 24053–24063.
[85] G.M. Vlăsceanu, H. Iovu, M. Ioniță, Graphene inks for the 3D printing of cell culture scaffolds and related molecular arrays, Compos. B Eng. 162 (2019) 712–723.
[86] C.-T. Huang, et al., A graphene–polyurethane composite hydrogel as a potential bioink for 3D bioprinting and differentiation of neural stem cells, J. Mater. Chem. B 5 (44) (2017) 8854–8864.
[87] X. Yu, T. Zhang, Y. Li, 3D printing and bioprinting nerve conduits for neural tissue engineering, Polymers 12 (8) (2020) 1637.
[88] M. Gasparotto, et al., 3D printed graphene-PLA scaffolds promote cell alignment and differentiation, Int. J. Mol. Sci. 23 (3) (2022) 1736.
[89] K. Gold, A.K. Gaharwar, A. Jain, Emerging trends in multiscale modeling of vascular pathophysiology: organ-on-a-chip and 3D printing, Biomaterials 196 (2019) 2–17.
[90] M. Hashemzaei, et al., Advances in stimuli-responsive hydrogels for tissue engineering and regenerative medicine applications: a review towards improving structural design for 3D printing, Curr. Pharmaceut. Des. 29 (40) (2023) 3187–3205.
[91] P.D. Costa, et al., Natural origin biomaterials for 4D bioprinting tissue-like constructs, Advanced Materials Technologies 6 (10) (2021) 2100168.
[92] N. Ashammakhi, et al., Advances and future perspectives in 4D bioprinting, Biotechnol. J. 13 (12) (2018) 1800148.
[93] T. Chen, Q. Qian, P. Makvandi, E.N. Zare, Q. Chen, L. Chen, Z. Zhang, H. Zhou, W. Zhou, H. Wang, X. Wang, Y. Chen, Y. Zhou, A. Wu, Engineered high-strength biohydrogel as a multifunctional platform to deliver nucleic acid for ameliorating intervertebral disc degeneration, Bioact. Mater. 25 (2023) 107–121.
[94] M. Alonzo, et al., Bone tissue engineering techniques, advances, and scaffolds for treatment of bone defects, Current opinion in biomedical engineering 17 (2021) 100248.
[95] P. Bertsch, et al., Self-healing injectable hydrogels for tissue regeneration, Chem. Rev. 123 (2023) 834–873.
[96] A.R. Armiento, et al., Functional biomaterials for bone regeneration: a lesson in complex biology, Adv. Funct. Mater. 30 (44) (2020) 1909874.
[97] S. Yousefiasl, et al., Bone regeneration, Electrically Conducting Polymers and Their Composites for Tissue Engineering (2023) 109–136.
[98] A. Pacifici, et al., Decellularized hydrogels in bone tissue engineering: a topical review, Int. J. Med. Sci. 15 (5) (2018) 492.
[99] M. Sharifi, et al., Criteria, challenges, and opportunities for acellularized allogeneic/xenogeneic bone grafts in bone repairing, ACS Biomater. Sci. Eng. 8 (8) (2022) 3199–3219.
[100] L. Daneshmandi, et al., Graphene-based biomaterials for bone regenerative engineering: a comprehensive review of the field and considerations regarding biocompatibility and biodegradation, Adv. Healthcare Mater. 10 (1) (2021) 2001414.
[101] H. Zhao, et al., Nanocomposite hydrogels for tissue engineering applications, Nanoscale 12 (28) (2020) 14976–14995.
[102] S. Yue, et al., Hydrogel as a biomaterial for bone tissue engineering: a review, Nanomaterials 10 (8) (2020) 1511.
[103] A. Bharadwaz, A.C. Jayasuriya, Recent trends in the application of widely used natural and synthetic polymer nanocomposites in bone tissue regeneration, Mater. Sci. Eng. C 110 (2020) 110698.
[104] Y. Zhao, et al., Supramolecular adhesive hydrogels for tissue engineering applications, Chem. Rev. 122 (6) (2022) 5604–5640.
[105] Z. Liu, et al., Electroactive biomaterials and systems for cell fate determination and tissue regeneration: design and applications, Adv. Mater. 33 (32) (2021) 2007429.
[106] S. Khan, et al., Fabrication strategies and biomedical applications of three-dimensional bacterial cellulose-based scaffolds: a review, Int. J. Biol. Macromol. 209 (2022) 9–30.
[107] H. Shen, et al., Acceleration of chondrogenic differentiation of human mesenchymal stem cells by sustained growth factor release in 3D graphene oxide incorporated hydrogels, Acta Biomater. 105 (2020) 44–55.
[108] Q. Wang, et al., A novel zwitterionic hydrogel incorporated with graphene oxide for bone tissue engineering: synthesis, characterization, and promotion of osteogenic differentiation of bone mesenchymal stem cells, Int. J. Mol. Sci. 24 (3) (2023) 2691.
[109] L.-B. Jiang, et al., Injectable sericin based nanocomposite hydrogel for multi-modal imaging-guided immunomodulatory bone regeneration, Chem. Eng. J. 418 (2021) 129323.
[110] D. Jiao, et al., Bidirectional differentiation of BMSCs induced by a biomimetic procallus based on a gelatin-reduced graphene oxide reinforced hydrogel for rapid bone regeneration, Bioact. Mater. 6 (7) (2021) 2011–2028.
[111] X. Zhou, et al., Three-dimensional printing biologically inspired DNA-based gradient scaffolds for cartilage tissue regeneration, ACS Appl. Mater. Interfaces 12 (29) (2020) 33219–33228.
[112] S. Murab, et al., Alginate Based Hydrogel Inks for 3D Bioprinting of Engineered Orthopedic Tissues, Carbohydrate Polymers, 2022 119964.
[113] F.S. Segundo, M. Sá, R. Souza, Cartilage tissue engineering and regeneration, in: Cartilage Tissue Engineering and Regeneration Techniques, IntechOpen, London, UK, 2019, pp. 1–14.
[114] N. Amiryaghoubi, et al., Application of graphene in cartilage-articular tissue engineering and chondrogenic differentiation, J. Drug Deliv. Sci. Technol. (2023) 104437.
[115] J. Li, et al., Advances of injectable hydrogel-based scaffolds for cartilage regeneration, Regenerative biomaterials 6 (3) (2019) 129–140.
[116] S.R. Shin, et al., Graphene-based materials for tissue engineering, Adv. Drug Deliv. Rev. 105 (2016) 255–274.
[117] Y. Hou, et al., Biomimetic construction of a lubricious hydrogel with robust mechanics via polymer chains interpenetration and entanglement for TMJ disc replacement, Chem. Eng. J. 460 (2023) 141731.
[118] X.-K. Fu, et al., Bioinspired hydroxyapatite coating infiltrated with a graphene oxide hybrid supramolecular hydrogel orchestrates antibacterial and self-lubricating performance, ACS Appl. Mater. Interfaces 14 (28) (2022) 31702–31714.
[119] C. Lyu, et al., Graphene hydrogel as a porous scaffold for cartilage regeneration, ACS Appl. Mater. Interfaces 14 (49) (2022) 54431–54438.
[120] M. Li, et al., Advances of hydrogel therapy in periodontal regeneration—a materials perspective review, Gels 8 (10) (2022) 624.
[121] Y. Zhu, L. Zhao, T. Ngai, Multiphasic membranes/scaffolds for periodontal guided tissue regeneration, Macromol. Mater. Eng. (2023) 2300081.
[122] S. Jepsen, et al., Regenerative surgical treatment of furcation defects: a systematic review and Bayesian network meta-analysis of randomized clinical trials, J. Clin. Periodontol. 47 (2020) 352–374.
[123] M. Samiei, et al., Bioactive hydrogel-based scaffolds for the regeneration of dental pulp tissue, J. Drug Deliv. Sci. Technol. 64 (2021) 102600.
[124] M. Vera-Sánchez, et al., Silk-fibroin and graphene oxide composites promote human periodontal ligament stem cell spontaneous differentiation into osteo/cementoblast-like cells, Stem Cell. Dev. 25 (22) (2016) 1742–1754.

[125] Y. Li, et al., Polydopamine-mediated graphene oxide and nanohydroxyapatite-incorporated conductive scaffold with an immunomodulatory ability accelerates periodontal bone regeneration in diabetes, Bioact. Mater. 18 (2022) 213–227.
[126] N. Amiryaghoubi, et al., Injectable thermosensitive hybrid hydrogel containing graphene oxide and chitosan as dental pulp stem cells scaffold for bone tissue engineering, Int. J. Biol. Macromol. 162 (2020) 1338–1357.
[127] B. Wang, et al., The preparation of lactoferrin/magnesium silicate lithium injectable hydrogel and application in promoting wound healing, Int. J. Biol. Macromol. 220 (2022) 1501–1511.
[128] Y. Liang, J. He, B. Guo, Functional hydrogels as wound dressing to enhance wound healing, ACS Nano 15 (8) (2021) 12687–12722.
[129] M. Li, et al., Hydrogel adhesives for generalized wound treatment: design and applications, J. Polym. Sci. 60 (8) (2022) 1328–1359.
[130] R. Yu, H. Zhang, B. Guo, Conductive biomaterials as bioactive wound dressing for wound healing and skin tissue engineering, Nano-Micro Lett. 14 (2022) 1–46.
[131] M.U.A. Khan, et al., Multifunctional arabinoxylan-functionalized-graphene oxide based composite hydrogel for skin tissue engineering, Front. Bioeng. Biotechnol. 10 (2022) 536.
[132] B. Xue, et al., Stretchable and self-healable hydrogel artificial skin, Natl. Sci. Rev. 9 (7) (2022) nwab147.
[133] P. Zhao, et al., Versatile hydrogel dressing with skin adaptiveness and mild photothermal antibacterial activity for methicillin-resistant Staphylococcus aureus-infected dynamic wound healing, Adv. Sci. (2023) 2206585.
[134] S. Vijayavenkataraman, Nerve guide conduits for peripheral nerve injury repair: a review on design, materials and fabrication methods, Acta Biomater. 106 (2020) 54–69.
[135] C. Chircov, et al., Natural, synthetic, and hybrid and composite biomaterials for neural tissue engineering, in: Biomaterials for Neural Tissue Engineering, Elsevier, 2023, pp. 21–58.
[136] C. Chen, et al., Bioinspired hydrogel electrospun fibers for spinal cord regeneration, Adv. Funct. Mater. 29 (4) (2019) 1806899.
[137] Y. Zhang, et al., Implantation of a functional TEMPO-hydrogel induces recovery from rat spinal cord transection through promoting nerve regeneration and protecting bladder tissue, Biomater. Sci. 8 (6) (2020) 1695–1701.
[138] W. Zhu, et al., Advances and progress in self-healing hydrogel and its application in regenerative medicine, Materials 16 (3) (2023) 1215.
[139] A. Rezaei, et al., Collagen/chitosan-functionalized graphene oxide hydrogel provide a 3D matrix for neural stem/precursor cells survival, adhesion, infiltration and migration, J. Bioact. Compat Polym. 36 (4) (2021) 296–313.
[140] X. Liu, et al., Functionalized carbon nanotube and graphene oxide embedded electrically conductive hydrogel synergistically stimulates nerve cell differentiation, ACS Appl. Mater. Interfaces 9 (17) (2017) 14677–14690.
[141] J. Amagat, et al., Self-snapping hydrogel-based electroactive microchannels as nerve guidance conduits, Materials Today Bio 16 (2022) 100437.
[142] E.A. Margolis, et al., Manufacturing the multiscale vascular hierarchy: progress toward solving the grand challenge of tissue engineering, Trends Biotechnol. 41 (2023) 1400–1416.
[143] X. Yan, H. Sun, P. Yang, Recent advances on electroconductive hydrogels used in heart repair and regeneration, Adv. Mater. Sci. Eng. (2022) 2022.
[144] G. Kougkolos, et al., Hydrogels with electrically conductive nanomaterials for biomedical applications, J. Mater. Chem. B 11 (10) (2023) 2036–2062.
[145] X. Ren, Z. Jiang, M. Tang, Application of conductive hydrogels in cardiac tissue engineering, STEMedicine 4 (2) (2023) e169-e169.
[146] J. Zhou, et al., Injectable OPF/graphene oxide hydrogels provide mechanical support and enhance cell electrical signaling after implantation into myocardial infarct, Theranostics 8 (12) (2018) 3317.
[147] J. Zhou, et al., ROS scavenging graphene-based hydrogel enhances type H vessel formation and vascularized bone regeneration via ZEB1/notch1 mediation, Macromol. Biosci. 23 (4) (2023) 2200502.
[148] A. Paul, et al., Injectable graphene oxide/hydrogel-based angiogenic gene delivery system for vasculogenesis and cardiac repair, ACS Nano 8 (8) (2014) 8050–8062.
[149] Z. Yuan, et al., Development and novel design of clustery graphene oxide formed Conductive Silk hydrogel cell vesicle to repair and routine care of myocardial infarction: investigation of its biological activity for cell delivery applications, J. Drug Deliv. Sci. Technol. 60 (2020) 102001.
[150] G. Choe, et al., Anti-oxidant activity reinforced reduced graphene oxide/alginate microgels: mesenchymal stem cell encapsulation and regeneration of infarcted hearts, Biomaterials 225 (2019) 119513.
[151] C. Chen, Y. Xi, Y. Weng, Progress in the development of graphene-based biomaterials for tissue engineering and regeneration, Materials 15 (6) (2022) 2164.
[152] S. Saghebasl, et al., Biodegradable functional macromolecules as promising scaffolds for cardiac tissue engineering, Polym. Adv. Technol. 33 (7) (2022) 2044–2068.
[153] A. Shariati, et al., Graphene-based materials for inhibition of wound infection and accelerating wound healing, Biomed. Pharmacother. 158 (2023) 114184.
[154] A. Williams, et al., Graphene-based materials in dental applications: antibacterial, biocompatible, and bone regenerative properties, International Journal of Biomaterials (2023) 2023.
[155] H.P. Ferreira, et al., Using graphene-based materials for stiff and strong poly (ethylene glycol) hydrogels, Int. J. Mol. Sci. 23 (4) (2022) 2312.
[156] H.M. El-Husseiny, et al., Smart/stimuli-responsive hydrogels: cutting-edge platforms for tissue engineering and other biomedical applications, Materials Today Bio 13 (2022) 100186.
[157] J. Hu, S. Liu, C. Fan, Applications of functionally-adapted hydrogels in tendon repair, Front. Bioeng. Biotechnol. (2023) 11.
[158] Y. Tang, et al., Functional biomaterials for tendon/ligament repair and regeneration, Regenerative Biomaterials 9 (2022).
[159] D. Bao, et al., Combination of graphene oxide and platelet-rich plasma improves tendon–bone healing in a rabbit model of supraspinatus tendon reconstruction, Regenerative Biomaterials 8 (6) (2021) rbab045.
[160] P.E.F. Barzegar, et al., Graphene-MoS2 polyfunctional hybrid hydrogels for the healing of transected Achilles tendon, Biomater. Adv. 137 (2022) 212820.
[161] J.P. Yoon, et al., Effects of a graphene oxide-alginate sheet scaffold on rotator cuff tendon healing in a rat model, J. Orthop. Surg. 30 (3) (2022) 10225536221125950.
[162] D. Yu, et al., Myogenic differentiation of stem cells for skeletal muscle regeneration, Stem Cell. Int. (2021) 2021.
[163] X. Jing, et al., Mussel-inspired electroactive chitosan/graphene oxide composite hydrogel with rapid self-healing and recovery behavior for tissue engineering, Carbon 125 (2017) 557–570.
[164] A. Patel, et al., Hierarchically aligned fibrous hydrogel films through microfluidic self-assembly of graphene and polysaccharides, Biotechnol. Bioeng. 115 (10) (2018) 2654–2667.
[165] J. Aparicio-Collado, et al., Electroactive calcium-alginate/polycaprolactone/reduced graphene oxide nanohybrid hydrogels for skeletal muscle tissue engineering, Colloids Surf. B Biointerfaces 214 (2022) 112455.
[166] T.T. Tung, et al., Recent advances in sensing applications of graphene assemblies and their composites, Adv. Funct. Mater. 27 (46) (2017) 1702891.
[167] M. Radulescu, et al., Advances in drug delivery systems, from 0 to 3D superstructures, Curr. Drug Targets 19 (4) (2018) 393–405.
[168] Y. Li, et al., Additive manufacturing high performance graphene-based composites: a review, Compos. Appl. Sci. Manuf. 124 (2019) 105483.
[169] R. Teixeira-Santos, et al., Graphene-based composites for biomedical applications: surface modification for enhanced antimicrobial activity and biocompatibility, Biomolecules 13 (11) (2023) 1571.
[170] E.I. Biru, et al., Graphene oxide–protein-based scaffolds for tissue engineering: recent advances and applications, Polymers 14 (5) (2022) 1032.
[171] L.M.T. Phan, et al., Graphene integrated hydrogels based biomaterials in photothermal biomedicine, Nanomaterials 11 (4) (2021) 906.
[172] P. Yu, et al., Self-assembled high-strength hydroxyapatite/graphene oxide/chitosan composite hydrogel for bone tissue engineering, Carbohydr. Polym. 155 (2017) 507–515.
[173] L. Wang, et al., Application of injectable silk fibroin/graphene oxide hydrogel combined with bone marrow mesenchymal stem cells in bone tissue engineering, Colloids Surf. A Physicochem. Eng. Asp. 604 (2020) 125318.
[174] H. Qin, et al., MicroRNA-29b/graphene oxide–polyethyleneglycol–polyethylenimine complex incorporated within chitosan hydrogel promotes osteogenesis, Front. Chem. 10 (2022).
[175] S. Saravanan, S. Vimalraj, D. Anuradha, Chitosan based thermoresponsive hydrogel containing graphene oxide for bone tissue repair, Biomed. Pharmacother. 107 (2018) 908–917.
[176] J. Lu, et al., Self-supporting graphene hydrogel film as an experimental platform to evaluate the potential of graphene for bone regeneration, Adv. Funct. Mater. 23 (28) (2013) 3494–3502.
[177] S. Pathmanapan, P. Periyathambi, S.K. Anandasadagopan, Fibrin hydrogel incorporated with graphene oxide functionalized nanocomposite scaffolds for bone repair—in vitro and in vivo study, Nanomed. Nanotechnol. Biol. Med. 29 (2020) 102251.
[178] X. Wang, et al., Photothermally triggered biomimetic drug delivery of Teriparatide via reduced graphene oxide loaded chitosan hydrogel for osteoporotic bone regeneration, Chem. Eng. J. 413 (2021) 127413.
[179] D. Li, et al., Self-assembled hydroxyapatite-graphene scaffold for photothermal cancer therapy and bone regeneration, J. Biomed. Nanotechnol. 14 (12) (2018) 2003–2017.
[180] V. Nazar, et al., Gelatin hydrogel reinforced by graphene oxide grafted chitosan for cartilage tissue engineering application, International Journal of Polymeric Materials and Polymeric Biomaterials (2022) 1–12.
[181] Y. Jiang, et al., Multifunctional load-bearing hybrid hydrogel with combined drug release and photothermal conversion functions, NPG Asia Mater. 12 (1) (2020) 18.
[182] A. Marrella, et al., Enhanced mechanical performances and bioactivity of cell laden-graphene oxide/alginate hydrogels open new scenario for articular tissue engineering applications, Carbon 115 (2017) 608–616.
[183] H. Shen, et al., Chondroinductive factor-free chondrogenic differentiation of human mesenchymal stem cells in graphene oxide-incorporated hydrogels, J. Mater. Chem. B 6 (6) (2018) 908–917.
[184] F. Olate-Moya, et al., Chondroinductive alginate-based hydrogels having graphene oxide for 3D printed scaffold fabrication, ACS Appl. Mater. Interfaces 12 (4) (2020) 4343–4357.
[185] Y. Meng, et al., In situ cross-linking of poly (vinyl alcohol)/graphene oxide–polyethylene glycol nanocomposite hydrogels as artificial cartilage replacement: intercalation structure, unconfined compressive behavior, and biotribological behaviors, J. Phys. Chem. C 122 (5) (2018) 3157–3167.
[186] M.F. Graça, et al., Reduced graphene oxide-enriched chitosan hydrogel/cellulose acetate-based nanofibers application in mild hyperthermia and skin regeneration, Int. J. Biol. Macromol. 229 (2023) 224–235.
[187] X. Pan, et al., A bionic tactile plastic hydrogel-based electronic skin constructed by a nerve-like nanonetwork combining stretchable, compliant, and self-healing properties, Chem. Eng. J. 379 (2020) 122271.

[188] W. Hanif, et al., Physically crosslinked PVA/graphene-based materials/aloe vera hydrogel with antibacterial activity, RSC Adv. 11 (46) (2021) 29029–29041.
[189] J. Hao, et al., An IFI6-based hydrogel promotes the healing of radiation-induced skin injury through regulation of the HSF1 activity, J. Nanobiotechnol. 20 (1) (2022) 1–14.
[190] H. Zhang, et al., A graphene hybrid supramolecular hydrogel with high stretchability, self-healable and photothermally responsive properties for wound healing, RSC Adv. 11 (11) (2021) 6367–6373.
[191] L. Chen, et al., Conducting molybdenum sulfide/graphene oxide/polyvinyl alcohol nanocomposite hydrogel for repairing spinal cord injury, J. Nanobiotechnol. 20 (1) (2022) 210.
[192] Q. Huang, et al., Aligned graphene mesh-supported double network natural hydrogel conduit loaded with netrin-1 for peripheral nerve regeneration, ACS Appl. Mater. Interfaces 13 (1) (2021) 112–122.
[193] M.C. McNamara, et al., Enhancing the conductivity of cell-laden alginate microfibers with aqueous graphene for neural applications, Frontiers in Materials 7 (2020) 61.
[194] K. Pradhan, et al., Neuro-regenerative choline-functionalized injectable graphene oxide hydrogel repairs focal brain injury, ACS Chem. Neurosci. 10 (3) (2018) 1535–1543.
[195] S. Aghajanian, et al., Facial nerve regeneration using silicone conduits filled with ammonia-functionalized graphene oxide and frankincense-embedded hydrogel, Inflamm. Regen. 41 (1) (2021) 13.
[196] S. Chen, et al., PAM/GO/gel/SA composite hydrogel conduit with bioactivity for repairing peripheral nerve injury, J. Biomed. Mater. Res. 107 (6) (2019) 1273–1283.
[197] N. Karimi Hajishoreh, et al., Reduced graphene oxide facilitates biocompatibility of alginate for cardiac repair, J. Bioact. Compat Polym. 35 (4–5) (2020) 363–377.
[198] Y. Liu, et al., Biocompatible, high-performance, wet-adhesive, stretchable all-hydrogel supercapacitor implant based on PANI@ rGO/Mxenes electrode and hydrogel electrolyte, Adv. Energy Mater. 11 (30) (2021) 2101329.
[199] J. Lee, et al., Nanoparticle-based hybrid scaffolds for deciphering the role of multimodal cues in cardiac tissue engineering, ACS Nano 13 (11) (2019) 12525–12539.
[200] J.H. Tsui, et al., Tunable electroconductive decellularized extracellular matrix hydrogels for engineering human cardiac microphysiological systems, Biomaterials 272 (2021) 120764.
[201] R. Si, et al., Human mesenchymal stem cells encapsulated-coacervated photoluminescent nanodots layered bioactive chitosan/collagen hydrogel matrices to indorse cardiac healing after acute myocardial infarction, J. Photochem. Photobiol. B Biol. 206 (2020) 111789.
[202] J. Park, et al., Micropatterned conductive hydrogels as multifunctional muscle-mimicking biomaterials: graphene-incorporated hydrogels directly patterned with femtosecond laser ablation, Acta Biomater. 97 (2019) 141–153.
[203] A. Khalili, et al., Self-actuating multilayer scaffold for skeletal muscle tissue engineering, Polym. Adv. Technol. 33 (10) (2022) 3228–3237.